Delft University of Technology
Faculty of Architecture & the Built Environment

THESIS

MSc GEOMATICS

EXPLORING THE POTENTIAL OF 5G POSITIONING VIA RSSI, COMPARING ITS EFFICACY WITH GNSS-RTK POSITIONING

Georgios Konstantinos (Akis) Nestoras

October 2024

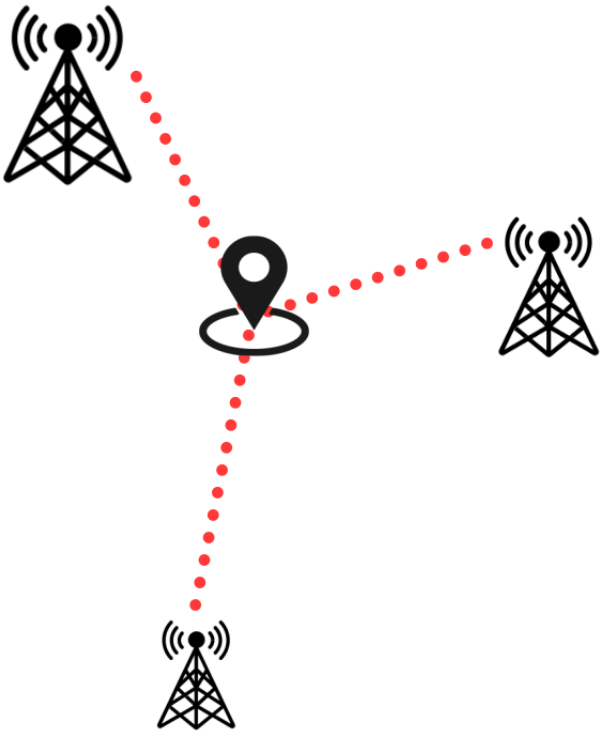

TU Delft Delft University of Technology

CGI

Delft University of Technology
Faculty of Architecture & the Build Environment

THESIS

MSc GEOMATICS

EXPLORING THE POTENTIAL OF 5G POSITIONING VIA RSSI, COMPARING ITS EFFICACY WITH GNSS-RTK POSITIONING

GEORGIOS KONSTANTINOS (AKIS) NESTORAS

October 2024

A thesis submitted to the Delft University of Technology in partial fulfillment of the requirements for the degree of Master of Science in Geomatics.

The work in this thesis was carried out in the: Geo-Database Management Center of Delft University of Technology and CGI.

Supervisors:	Ir. Edward Verbree Dr.ir. B.M. (Martijn) Meijers
External Supervisor CGI:	Ir. Robert Voûte
Co-reader:	Dr.ir. F.J. (Freek) van Leijen

Abstract

Accurate positioning has become an essential component of modern life, crucial for applications ranging from navigation and industrial operations to emergency response. The Global Navigation Satellite System (GNSS) has traditionally provided reliable positioning, but its effectiveness diminishes in environments where satellite signals are obstructed, such as dense urban areas and indoor spaces. This thesis explores the potential of Fifth-Generation (5G) wireless communication technology, specifically utilizing Received Signal Strength Indicator (RSSI) data for positioning, as an alternative to GNSS.

The research investigates the effectiveness of 5G positioning through trilateration and compares it with GNSS-Real-Time Kinematic (RTK) positioning. The study aims to validate the accuracy and the reliability of 5G positioning and various real-world scenarios, focusing on challenging environments. Key aspects examined include the impact of topography on positioning accuracy and the influence of network distribution on Position Dilution of Precision (PDOP).

By attaching a 5G modem to a laptop, field measurements were collected and analyzed against the "ground truth" provided by GNSS-RTK. The results demonstrate the potential of 5G RSSI-based positioning to serve as a robust positioning solution. This study's findings hold significant relevance for the geomatics community, with implications for urban planning, infrastructure development, environmental monitoring, and disaster management.

Through critical analysis and validation, this thesis contributes to the advancement of positioning technologies, highlighting the limitations of 5G trilateration using RSSI, yet proposing it as a potential complement to GNSS. The findings pave the way for future research and practical applications in enhancing precise positioning systems.

Acknowledgements

I would like to express my deepest gratitude to the individuals and institutions that have supported me throughout the journey of completing my thesis.

First and foremost, I would like to thank my supervisors, Ir. Edward Verbree, Dr.ir. B.M. (Martijn) Meijers, and Ir. Robert Voûte. Ir. Verbree's expertise and unwavering support provided a strong foundation for my research. Dr.ir. Meijers' meticulous attention to detail and constructive criticism pushed me to refine my work continually. I am particularly grateful to Ir. Robert Voûte, Vice President of the Geo-ICT department at *CGI* in Rotterdam, for providing me with the invaluable opportunity to complete my thesis at such a prestigious company. His support and guidance were instrumental in shaping my research experience and allowed me to benefit from the extensive resources and expertise available at *CGI*.

I am also grateful to Dr.ir. F.J. (Freek) van Leijen for his role as the co-reader. His valuable insights and constructive comments greatly enhanced the quality of this thesis. I would also like to extend my sincere thanks to *Ericsson* for their support. I am deeply appreciative of Dr. Maciej Muehleisen, whose expertise as a leading 5G researcher was instrumental in explaining the complex aspects of 5G technology that I needed for my research. Additionally, I would like to thank Edwin Dijkstra, solution architect at *Ericsson*, for his assistance with the equipment.

I want to express my gratitude to my colleagues, friends, and teammates for their invaluable support and collaboration, which helped me through challenging moments. Last but not least, I extend my heartfelt thanks to my family for their unwavering support and love, which have been a constant source of strength and motivation.

Thank you all for your contributions, support, and encouragement. This thesis would not have been possible without you.

Contents

List of Figures

Acronyms

3GPP	3rd Generation Partnership Project
5G	Fifth-Generation
AGNSS	Augmented GNSS
AOD	Angle of Departure
AOA	Angle of Arrival
AP	Access Point
CID	Cell-Identity
DL	Downlink
DL-AoD	Downlink Angle of Departure
DL-TDOA	Dowlink Time Difference of Arrival
DOP	Dilution of Precision
eMBB	Enhanced Mobile Broadband
EPSG	European Petroleum Survey Group
FR	Frequency Range
FSPL	Free Space Path Loss
GIS	Geographic Information System
GNSS	Global Navigation Satellite System
GPS	Global Positioning System
HDOP	Horizontal Dilution of Precision
IoT	Internet of Things
LiDAR	Light Detection And Ranging
LOS	Line-of-Sight
LTE	Long Term Evolution
MC-RTT	multi-cell round trip time
MIMO	multiple-input multiple-output
mmWave	millimeter-Wave
NTRIP	Networked Transport of Real Time Configuration Management (RTCM) via Internet Protocol
NR	New Radio
NSA	Non-Standalone
OSR	Observation Space Representation
PDOP	Position Dilution of Precision
PCI	Physical Cell ID
QGIS	Quantum Geographic Information System
QMI	Qualcomm MSM Interface
RD	Rijksdriehoekscoördinaten
RP	Reference Point
RSSI	Received Signal Strength Indicator
RSRP	Reference Received Signal Power

RSRQ	Reference Signal Received Quality
RTCM	Real Time Configuration Management
RTK	Real-Time Kinematic
RTT	Round Trip Time
SA	standalone
SIM	Subscriber Identity Module
SINR	Signal to Interference Noise Ratio
SRS	Sounding Reference Signal
SSR	State Space Representation
TDoA	Time Difference of Arrival
TDOP	Time Dilution of Precision
TMF	Transmission Measurement Function
ToA	Time of Arrival
UE	User Equipment
UL	Uplink
UP-AoA	Uplink Angle of Arrival
VDOP	Vertical Dilution of Precision
UERE	User Equivalent Range Error

Chapter 1

Introduction

1.1 Motivation and Problem Statement

In today's interconnected world, the ability to pinpoint one's position accurately has become vital across various aspects of daily life, spanning transportation, industrial operations (e.g. autonomous vehicles for agricultural applications), emergency response, and beyond. Whether navigating through intricate urban landscapes or locating missing individuals during natural disasters, the importance of precise positioning cannot be overstated.

The advent of the Global Navigation Satellite System (GNSS) revolutionized the way we define our position, offering swift and accurate location data through the utilization of satellite signals. However, GNSS is not impervious to limitations, particularly in environments where LOS to satellites is obstructed, such as dense urban areas or indoor spaces. GNSS is also vulnerable to spoofing and jamming, which can compromise the reliability and accuracy of the location data (Humphreys et al., 2008).

The introduction of 5G wireless communication technology promises a paradigm shift in positioning capabilities. With its extensive coverage and ability to propagate signals through obstacles, 5G presents itself as a compelling alternative for determining position, complementing or even surpassing the capabilities of GNSS in certain scenarios. Utilizing 5G positioning technology could also detect spoofing and jamming in GNSS systems, and significantly enhance the national defence strategies.

The focus of this thesis project lies in exploring the potential of 5G positioning via Received Signal Strength Indicator (RSSI), comparing its efficacy with GNSS-Real-Time Kinematic (RTK) positioning. By leveraging RSSI data from 5G networks, the aim is to achieve accurate and reliable positioning even in challenging environments where GNSS signals may falter.

Through this comparative study, the goal is to validate the effectiveness of 5G positioning, assessing its precision, latency, reliability and practical utility across diverse real-world scenarios.

1.2 Scientific & Social Relevance

Incorporating RSSI data potentially allows accurate positioning, particularly in challenging environments like urban areas and indoor spaces where traditional GNSS signals may be attenuated or obstructed. By analyzing these RSSI measurements from multiple antennas and employing advanced algorithms, it is possible to find the device's position relative to the known locations of the base stations or access points.

Geomatics, with its focus on spatial data collection, analysis, and visualization, stands to benefit greatly from advancements in positioning technologies. By specifically investigating the trilateration method using the RSSI of 5G signals, this research offers a novel approach to overcoming the limitations of traditional positioning systems, particularly in urban environments with complex topographies. Geomatics professionals rely on accurate positioning data for a wide range of applications, from urban planning and infrastructure development to environmental monitoring and disaster management. Thus, the findings of this study hold considerable scientific relevance for the geomatics community.

The social relevance of this research is highlighted by its potential to enhance emergency response systems, such as E911 calls, by providing location approximations in areas where GNSS reception is poor or unavailable. Accurate positioning information is crucial during emergencies, enabling first responders to quickly locate individuals in need of assistance and potentially save their lives. This technology can also enhance public safety, assist in managing large-scale events and disasters and improve accessibility for individuals with disabilities especially indoors where there is no GNSS reception.

1.3 Research Objectives

In this study, literature's focus has been the world of 5G networks and how they might help in order to figure where the position of a certain device is. Instead of using traditional methods like Global Positioning System (GPS), the objective of this project is the exploration of the trilateration technique using just the signal strength of 5G signals. With this objective in consideration, the following primary research question emerges:

To what extent can the trilateration method for positioning, utilizing only the RSSI of the 5G network, serve?

The subquestions to be addressed in this research are:

1. *What is the potential accuracy of standalone 5G positioning with the trilateration method in comparison to the 'ground truth' given by GNSS-RTK solution?*
2. *What is the impact of topographic factors (e.g., buildings, urban canyons) on the accuracy of 5G positioning?*
3. *How is the PDOP affected by the distribution of the 5G network?*

1.4 Scope

The project's scope is about finding the outdoor position of a device using the 5G non-standalone network. Practical aspects of the project refer to attaching a regular 5G modem with multiple antennas to a laptop in order to assess the signal reception and through that define its position as well as get precise positioning with a GNSS-RTK device. These tools enable evaluating the system's performance within the cellular network, assessing signal strength and stability. The positioning algorithm that was used relies on trilateration using RSSI for determining position. Validation of position estimates is done against known "ground truth" using GNSS-RTK.

CGI is intrigued by this thesis project due to the challenges associated with relying mostly on GNSS for positioning, including issues like availability in obstructed areas, accuracy concerns, and susceptibility to jamming and spoofing. They are interested in 5G positioning as it

presents an alternative solution with wider coverage and potential improvements in reliability and resistance to spoofing. By integrating 5G positioning with GNSS, CGI aims to overcome the limitations of traditional positioning systems, ensuring dependable and precise location data for their applications and clients.

1.5 Thesis Outline

Chapter 2 provides the fundamental theoretical framework necessary for comprehending the subject matter with ease. It describes 5G and its associated possibilities, alongside an exposition of the principal positioning techniques. The trilateration method is elucidated in greater detail. Furthermore, the FSPL model is described, accompanied by an explanation of the signal propagation parameters that influence its effectiveness. Lastly, GNSS-RTK is discussed, including an exploration of potential errors that could impact its performance. This chapter also outlines the research conducted and discusses various alternatives considered for incorporation into the methodology of the project.

Chapter 3 details the process of estimating RSSI errors and their effect on position accuracy. It also explains the procedure for acquiring field measurements and describes the preliminary testing conducted. Finally, it discusses the final step of implementing the trilateration method.

Chapter 4 presents the outcomes derived from the implementation of the positioning algorithm and provides an analysis thereof.

Chapter 5 expands upon the insights garnered throughout this thesis, employing critical analysis to address the sub questions and the main research question. Additionally, recommendations are offered regarding potential avenues for future research.

Chapter 2

Theoretical Background & Related Work

There are multiple methods available for determining the location of a target within a given area, each leveraging different techniques and technologies. These methods include the Cell-Identity (CID) method, which relies on identifying the radio coverage area; angle-based positioning, which uses angular measurements of radio signals; trilateration, which calculates distances between transmitters and receivers; and fingerprinting, which matches signal strength data to a pre-established database. Many of these methods can be integrated with 5G technology to enhance positioning accuracy and efficiency. The following sections describe each of these techniques in detail.

2.1 5G and Possibilities

The precision in locating devices facilitated by 5G cellular networks opens up numerous commercial opportunities across various sectors such as transportation, public safety, retail, and healthcare. Compared to previous generations of communication technologies like Long Term Evolution (LTE), 5G introduces New Radio (NR) access technology. Offering advantages for precise positioning as standardized by 3rd Generation Partnership Project (3GPP), is a global collaboration defining mobile communication standards for interoperability and compatibility in Release 16. It is stated that 5G NR access technology, meets diverse metrics for Enhanced Mobile Broadband (eMBB), low-latency communication, and massive machine-type communication (Pileggi et al., 2023 & Cardoso et al., 2020).

The methods for 5G positioning utilize different measurements associated with user equipment, including angular measurements like Uplink Angle of Arrival (UP-AoA) or Downlink Angle of Departure (DL-AoD), and distance-based measurements such as Time of Arrival (ToA), Time Difference of Arrival (TDoA), Round Trip Time (RTT), and multi-cell round trip time (MC-RTT). These methods are implemented in various modes including User Equipment (UE)-assisted, UE-based, stand-alone, and network-based (Alghisi and Biagi, 2023 & Elshaer et al., 2014 & Pileggi et al., 2023).

Frequency Range (FR) 1 is a high-frequency range that is used for 5G deployment. It ranges from 24.3 GHz to 52.6 GHz in addition to FR 2, which covers frequencies below 7 GHz. Thanks to these bands, is used to overcome the challenge of limited spectrum availability in wireless communication, enabling high data rates, capacity, and bandwidth with minimal latency. It also ensures superior positioning accuracy. Radio signals within this frequency range experience penetration and diffraction losses, resulting in a predominant LOS element

and reduced multipath effects. Although millimeter-wave wireless signals have advantages, they also present challenges such as high path loss. However, these challenges can be addressed through the adoption of specialized compensation techniques like beamforming and highly directional antennas (Alimi et al., 2020 & Pileggi et al., 2023).

NR provides a crucial improvement in comparison to LTE, by providing up to 100 MHz in FR1 and 400 MHz in FR 2, at the same time that LTE supports a maximum of 20MHz. The variability in delay estimation is inversely related to signal bandwidth. This means that as signal bandwidth increases, the uncertainty in delay estimation decreases due to the narrowing of the main lobe in the correlation function. A narrower lobe makes it easier for the receiver to discriminate, leading to improved differentiation between direct and reflected paths (Pileggi et al., 2023 & Alimi et al., 2020).

Massive multiple-input multiple-output (MIMO) refers to the utilization of base stations with numerous antennas leading to potential interference challenges. These interference issues can be effectively addressed by employing beamforming (Talvitie et al., 2018). Beamforming is a strategic process that shapes the radiated beam patterns of antennas by consolidating processed signals towards intended terminals while nullifying interfering signal beams. The use of beamforming optimizes the energy consumption of the system, enhances the overall data transmission capacity and contributes to increased system security by mitigating interference. Moreover, beamforming proves to be well-suited for millimeter-Wave (mmWave) bands, demonstrating its versatility across different frequency ranges (E. Ali et al., 2017).

2.2 Positioning Methods

Cell-Identity-Based (CID)

The Cell-Identity (CID) method, also known as the proximity-based method is used in order to determine whether an object is located in a specific radio coverage area. To estimate this location, essentially the service base station's location should be known as well as the area of the serving cell that is utilised. The estimated area of the object is the intersection of these coverage areas as shown in Figure 2.1. For more effective results, a considerable amount of base stations needs to be deployed (Liu et al., 2017 & Mogyorósi et al., 2022).

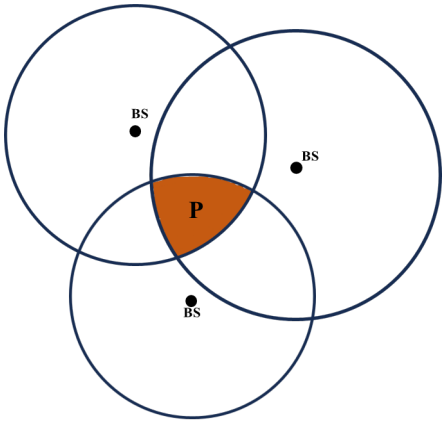

Figure 2.1: Cell-Identity-based positioning method figure illustrating the estimated object location as the intersection of the radio coverage areas of all the base stations.

Angle-Based

The Angle-based positioning is a technique used to determine the position of a target in a given space by leveraging angle measurements of the received radio signals as depicted in Figure 2.2. In this method, the angles between the target and known reference points are measured. By triangulating these angle measurements, the system can calculate the target's location (Liu et al., 2017 & Mogyorósi et al., 2022).

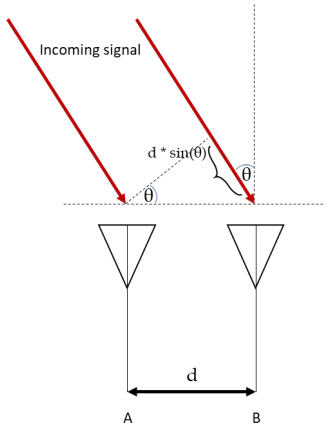

Figure 2.2: Angle of Arrival (AOA) positioning method using received radio signals. The target's location is determined by measuring the angles between the received radio signals and known reference points, followed by triangulation.

Trilateration

The trilateration method relies on measuring the distance between transmitters and a receiver. Its goal is to determine the unknown location of the user equipment. To achieve this, measurements involve the extraction of any kind of information to calculate the distances between the observation point and the transmitters. If the distances to at least three transmitters are known, the receiver's position can be uniquely determined, as shown in Figure 2.3. (Liu et al., 2017 & Mogyorósi et al., 2022).

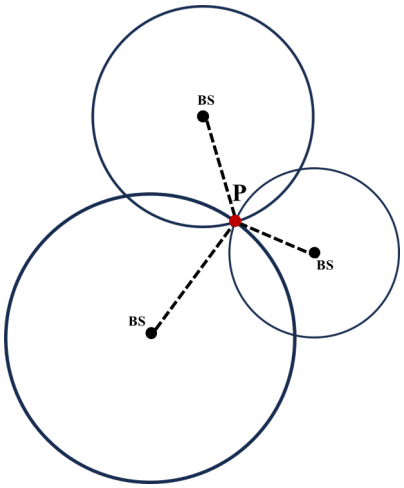

Figure 2.3: Trilateration positioning method illustrating the intersection of 3 circles at point P. The calculated distances from the observation point to the base stations BS form the radius of each circle. The unique position of the observation point P is determined by the intersection of these circles, where the radius of each circle intersects with the other 2.

Fingerprinting

Fingerprinting refers to the measurements of the signal strength of different Access Points (APs) at known Reference Points (RPs) to determine the user's location. The first phase of the method is the offline, where the fingerprint database is created according to the collection of signal strength data at various RPs. The online phase utilizes real-time signal strength measurements from the mobile device, employing at the same time specific matching algorithms to identify the closest fingerprint match in the database. The location information associated with the matched fingerprint reveal the user's location (Xia et al., 2017 & Liu et al., 2017 & Mogyorósi et al., 2022). Figure 2.4 demonstrates the steps of the method.

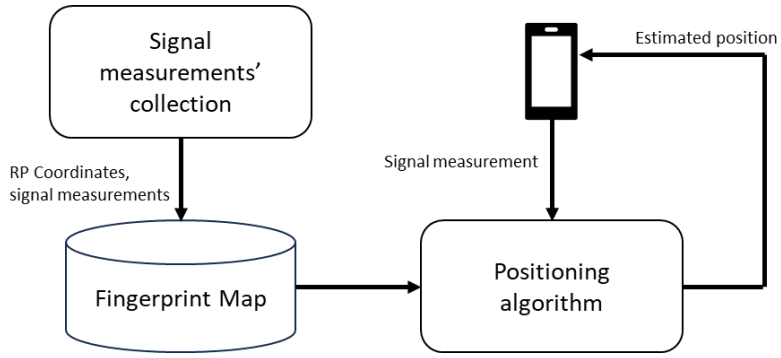

Figure 2.4: Fingerprinting positioning method demonstrating the offline and online phases. Signal measurements are collected from various APs at known RPs during the offline phase to create the fingerprint map/database. In the online phase, real-time signal measurements are matched against the database using a positioning algorithm to estimate the user's location.

Many of the positioning methods mentioned above, can be implemented with 5G technology. Its observations can be transmitted either from the user to the base stations (uplinked) or from the base stations to the user (downlinked). Figure 2.5 summarizes these methods (Alghisi and Biagi, 2023 & Keating et al., 2019).

Method	Description
DL-TDOA: Downlink Time Difference of Arrival	Based on Time of Arrival (TOA) measurements of Downlink signals received from multiple base stations (BSs) to user equipment. Computed quantities: - OTDOA: Observed Time Difference of Arrival -RTD: Real Time Difference -GTD: Geometric Time Difference
DL-AOD: Downlink Angle of Departure	Based on Reference Signal Received Power (RSRP) measurements performed by user. User requires assistance data from the network: a list of candidate base stations (BSs), BSs' geographical locations and beam information.
UL-TDOA: Uplink Time Difference of Arrival	User's signal is received by multiple base stations (BSs), which compute the Time of Arrival (TOA). Measurements have a common time scale and are called Uplink-Relative Time of Arrival (UL-RTOA). Then, they are sent to the location management function (LMF), which computes the Time Difference of Arrival (TDOA).
UL-AOA: Uplink Angle of Arrival	The receivved signal from the user is transformed by gNodeB (gNB) in azimuth and elevation, and directional antennas are required, implying the network-based mode.
RTT: Round Trip Time	Uses two-way Time of Arrival measurements and requires no base station (BS) synchronization.
MC-RTT: Multi-cell Round Trip Time	Estimate Round-Trip-Time between multiple gNBs, requires both Uplink (UL) and Downlink (DL). No synchronization erros.

Figure 2.5: 5G positioning methods in a nutshell (Alghisi and Biagi, 2023).

The 5G positioning methods that were introduced in Release 16 of 3GPP are explained in

more detail below.

Downlink Time Difference of Arrival (DL-TDOA)

Dowlink Time Difference of Arrival (DL-TDOA) is a positioning technique where the receiver measures the difference in arrival times of Downlink (DL) signals from multiple base stations. This is typically achieved by comparing the timing of reference signals, from these base stations. Then, the receiver reports these reference signal time differences to the network's location server. Using known positions of the base stations and the reference signal time differences' measurements, the location server calculates the position of the receiver.

Downlink Angle of Departure (DL-AoD)

The Downlink Angle of Departure (DL-AoD) utilizes the RSRP reports from the receiver to determine the Angle of Departure (AOD) from multiple base stations, enabling triangulation of the receiver based on these. More specifically, it refers to the angle at which signals are transmitted from the base station to the user device, departing from the base station antennas.

Uplink Time Difference of Arrival (UL-TDOA)

In this case, the receiver transmits a Sounding Reference Signal (SRS) that is received by multiple base stations. Using the New Radio (NR) measurement function that was introduced in 3GPP Release 16 called Transmission Measurement Function (TMF), the measurement of the relative Time of Arrival (ToA) is computed and transmitted to the location server. The receiver's position is then calculated based on the relative ToA measurements of the signals of all the base stations.

Uplink Angle of Arrival (UL-AoA)

The Sounding Reference Signal (SRS) is utilized as the reference signal for measuring the Angle of Arrival (AOA). The receiver transmits SRS signals to the base station periodically. By analyzing the received SRS signals at the base station, the network can estimate the AOA of the incoming signals. This involves processing the signal to determine its phase and amplitude characteristics relative to the antenna array, enabling the calculation of the angle of arrival.

Multi-cell Round Trip Time (MC-RTT)

Multi-cell Round Trip Time (MC-RTT) method is similar to the other time-related techniques. However, the main difference of this method is that it utilizes both the Downlink (DL) and Uplink (Uplink (UL)) received signal in order to perform the trilateration and estimate the receiver's position. The increased the total cost should be considered as a big disadvantage, but using MC-RTT the synchronization errors are avoided.

2.3 Free Space Path Loss (FSPL)

During the transmission of radio or electromagnetic waves in open space, wireless communication can be affected by many loss mechanisms such as attenuation, reflections and refractions. One of them is FSPL which is the reduction of the signal strength along a direct LOS path through open space. This type of loss is proportional to the square of the distance

separating the transmitter and the receiver, as well as the square of the frequency of the radio signal. The Equation that describes this expression mathematically is shown below (Ahmad et al., 2019 & Islam and Haider, 2010):

$$\begin{aligned} \mathrm{FSPL(dB)} &= 10\log_{10}\left(\left(\frac{4\pi d_{\mathrm{m}} f_{\mathrm{Hz}}}{c}\right)^2\right) - \mathrm{G_t} - \mathrm{G_r} \\ &= 20\log_{10}(d_{\mathrm{m}}) + 20\log_{10}(f_{\mathrm{Hz}}) + 20\log_{10}\left(\frac{4\pi}{c}\right) - \mathrm{G_t} - \mathrm{G_r} \\ &= 20\log_{10}(d_{\mathrm{m}}) + 20\log_{10}(f_{\mathrm{Hz}}) - 147.55 - \mathrm{G_t} - \mathrm{G_r}. \end{aligned} \tag{2.1}$$

where f is the frequency, d is the distance between the transmitter and the receiver, c is the speed of light, G_t is the gain of the transmitting antenna and and G_r the gain of the receiver in dB. Utilizing SI units, d is measured in meters, f in hertz s^{-1}, and c in meters per second $(\frac{\mathrm{m}}{\mathrm{s}})$. In a vacuum, the speed of light c is $299,792,458\,\frac{\mathrm{m}}{\mathrm{s}}$.
For typical radio applications, it is common to find d measured in kilometers and f in gigahertz, in which case the FSPL Equation becomes:

$$\mathrm{FSPL(dB)} = 20\log_{10}(d_{\mathrm{km}}) + 20\log_{10}(f_{\mathrm{GHz}}) + 92.45 - \mathrm{G_t} - \mathrm{G_r} \tag{2.2}$$

The relation between RSSI and FSPL is given by the Equation:

$$\mathrm{RSSI(dB)} = \mathrm{Tx\_Power} + \mathrm{G_t} + \mathrm{G_r} - \mathrm{FSPL} \tag{2.3}$$

where Tx_Power is the transmitted power in dBm. So, that means that:

$$\mathrm{RSSI(dB)} = \mathrm{Tx\_Power} + \mathrm{G_t} + \mathrm{G_r} - (20\log_{10}(d_{\mathrm{km}}) + 20\log_{10}(f_{\mathrm{GHz}}) + 92.45)$$

and if someone solve this Equation for distance:

$$d_{\mathrm{km}} = 10^{\left(\frac{\mathrm{Tx\_Power}+\mathrm{G_t}+\mathrm{G_r}-\mathrm{RSSI}-20\log_{10}(\mathrm{f_{GHz}})-92.45}{20}\right)} \tag{2.4}$$

However, the idea of multiplying the $\log_{10}(d_{\mathrm{m}})$ with 20 (10×2) is only valid for omnidirectional free-space propagation. The 5G antennas are not omnidirectional, so in this case, it will be a different value than 2.

The following example (Figure 2.6) illustrates the RSSI values at various distances for a given set of random parameters. The frequency is considered to be 2.4 GHz, the transmitter gain 17 dB, the receiver gain 4 dB and the distances ranging from 1 meter to 1000 meters. The power that is transmitted is considered 16.3 dBm.

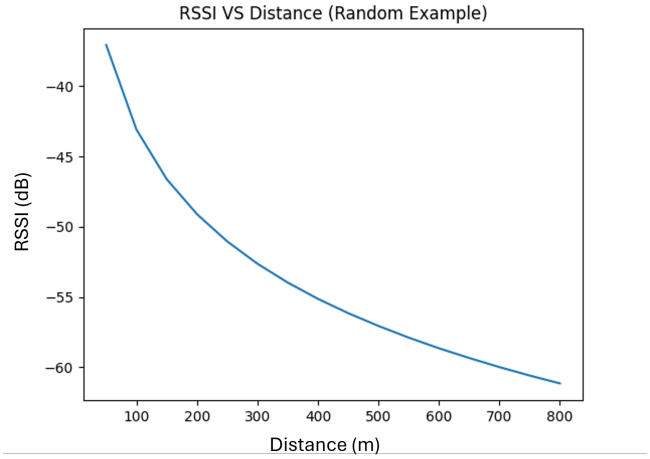

Figure 2.6: FSPL diagram illustrating the variation in RSSI from -35 dBm to -65 dBm as the distance increases from 50 meters to 800 meters.

2.4 Signal Propagation Parameters

There is a variety of factors that influence 5G signal propagation due to its use of of higher frequency in comparison to previous generations of mobile networks. These factors include natural and artificial elements in the environment that cause signal reflections, diffractions and attenuations. Key topographic factors include trees, buildings, terrain elevation, and other obstacles. Vegetation, especially trees, can have a profound effect on 5G signal accuracy since they their leaves, branches and trunks tend to absorb and scatter the signal, reducing its strength as it passes through. The most common effects are (Speidel, 2021 & S. Ali et al., 2024) :

- **Reflection**: 5G signals can reflect off certain surfaces like glass, metal, or buildings. This can create multiple signal paths which can either improve or degrade the signal quality depending on the interference patterns.
- **Diffraction**: This occurs when a 5G signal bends around obstacles such as edges of buildings or other structures. Diffraction allows signals to reach areas that are not in the direct line of sight of the transmitter.
- **Interference**: Interference from other electronic devices, overlapping signals from other 5G cells, or from different communication systems can degrade the quality of the signal.
- **Shadowing**: Large obstacles such as buildings can create shadow zones where the signal is significantly weakened or completely blocked. That is why proper network distribution is need so as adequate coverage is ensured.
- **Penetration Loss**: Higher frequency 5G signals have greater difficulty penetrating through solid objects like walls, buildings, and even trees. This results in signal attenuation and can significantly reduce indoor coverage unless complemented by indoor small cells or other solutions.
- **Scattering**: Scattering happens when the 5G signal encounters small objects or rough surfaces, causing the signal to scatter in multiple directions. This effect can be caused by foliage, street furniture, and other small-scale obstructions.

- **Multipath Propagation**: Due to reflection, diffraction, and scattering, 5G signals often take multiple paths to reach the receiver. These multiple paths can cause constructive or destructive interference, leading to signal fading, which can impact the reliability and quality of the signal.

2.5 Real-Time Kinematic (RTK)

RTK is a technique used to improve the accuracy of a standalone GNSS receiver. RTK is an advanced positioning method surpassing standard GPS accuracy, which is two to four meters. Unlike conventional GPS, which relies on pseudo-random codes, RTK utilizes carrier waves for more precise measurements (Hexagon, 2023).

Two GNSS receivers are utilised in RTK, a base station and the user's GNSS receiver, also known as the rover. In this method, a GNSS base station is positioned at a fixed location, and both the base station and the user's GNSS receiver simultaneously gather GNSS observations. The base station then transmits its observations, including pseudo-range and carrier-phase data, along with its accurate position, to the user through a suitable communication link (Feng and Wang, 2008). The user's GNSS receiver uses this correction data to improve its own computed position from the GNSS and then it is able to achieve centimeter precision.

By incorporating GNSS carrier-phase observations and ambiguity resolution, RTK positioning achieves centimeter-level accuracy in open-sky scenarios. However, its performance faces challenges in deep urban environments where the accuracy requirements for dynamic systems are not consistently met. In such settings, buildings can obstruct, weaken, reflect, and diffract GNSS signals, leading to insufficient visible satellites and observations affected by severe multipath effects. This limits RTK's effectiveness in delivering high-precision positioning in urban landscapes (Feng and Wang, 2008).

Figure 2.7 illustrates the GNSS-RTK system, showing how both the positioning device and the RTK server receive signals from GNSS satellites. The RTK server processes these signals to provide correction information to the positioning device, enhancing its positional accuracy.

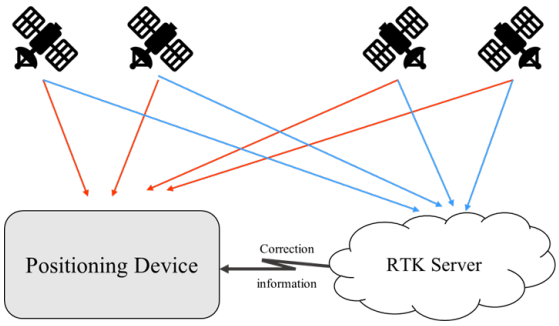

Figure 2.7: GNSS - RTK system where the positioning device and RTK server both receive signals from GNSS satellites; the RTK server processes these signals to provide correction information to the positioning device, enhancing its positional accuracy.

2.6 Real-Time Kinematic (RTK) Errors

Pseudo-range is derived from the observed travel time of a signal transmitted from a satellite to a receiver, multiplied by the speed of light. This measurement, however, is susceptible to various sources of error such as satellite orbit and clock discrepancies, biases in satellite and

receiver hardware, and atmospheric effects, specifically ionospheric and tropospheric influences. Providers of GNSS augmentation services generate corrections in real-time by constantly monitoring signals received from reference stations (Geo++, 2023).
GNSS positioning accuracy is affected by several types of error (Groves, 2013):

- Ionospheric errors: as the signal "travels" through the ionosphere, the conditions of it and its density of electrons can play a significant role in the signal propagation.
- Tropospheric errors: GNSS signals are delayed while passing throughout the troposphere depending on the different heights of the earth's surface. That is why, very high height difference between the base stations and the rover is not ideal.
- Signal obstructions: the number of visible satellites is reduced when an obstacle exists leading to reduced GNSS performance. Also, different types of materials and surfaces such as glass, can reflect the signal and affect the travel time of it.
- Geometric configuration of satellites: GNSS design is based on autonomous code observation with worldwide coverage, ensuring the visibility of at least four satellites positioned above 5°all time. A deficient satellite arrangement (distribution as perceived by the observer) results in elevated Dilution of Precision (DOP). Moreover, for 3D positioning, having at least four observable satellites is essential when relying on phase observations. So, when brief interruptions exist, then Real-Time Kinematic (RTK) measurements become impracticable with a single GNSS system.
- Other errors: satellites transmit to the GNSS receivers information for their clock offsets and orbits.

For these corrections there are two types of representations that provide different qualities, the Observation Space Representation (OSR) and the State Space Representation (SSR) (Chen et al., 2023 & Verbree, 2023).

More specifically, the objective of OSR is the creation of virtual GNSS reference stations by interpolating observations of multiple GNSS reference stations (Geo++, 2023). The total GNSS error for the carrier phase observations is an aggregate of distance-dependent errors. In RTK-networking, an inherent uncertainty exists, referred to as the representation error, influenced by the irregular physical conditions between the real reference stations. This error persists unless the distance between the stations is reduced and cannot be mitigated (Chen et al., 2023 & Wabbena et al., 2005).

On the other hand, in SSR all the the individual GNSS error components are estimated as state parameters. These real-time parameters are sent to the rover, allowing the user to refine their observations from a singular GNSS receiver. By using the SSR corrections that are specific to their individual position, RTK positioning is conducted based on the adjusted observations (Chen et al., 2023 & Wabbena et al., 2005).

The utilization of high-speed cellular networks such as LTE or 5G leads to the share of data in order to improve the accuracy of location information of single devices. The integration of GNSS correction data with other capabilities of the cellular network to enhance location-related services can take place in order to regularly update a server with information about where a device is located, to use the cellular network to independently confirm and validate the accuracy of the location information provided by GNSS and most importantly, to determine a device's location using methods that rely on the characteristics of the specific radio access network, such as 5G, for improved precision (Gunnarsson and Shreevastav, 2022).

2.7 Distance Measurements

In certain steps of this study, it is necessary to calculate the distance between a 5G cell tower, with coordinates provided by *Vodafone Ziggo*'s Excel file (see Appendix A.4), and an observation point, whose coordinates are obtained using the GNSS-RTK device (see Section 3.3). The algorithm for computing this distance is detailed in this Section.

The line segment that connects the points i and j defines the Euclidean distance between these two points (Figure 2.8). Mathematically, it is given by Equation 2.5 (Tiberius et al., 2022):

$$E(l_{ij}) = \sqrt{(x_j - x_i)^2 + (y_j - y_i)^2} \tag{2.5}$$

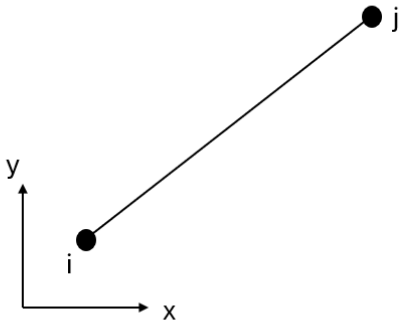

Figure 2.8: Distance measurement in 2D between points i and j (Tiberius et al., 2022)

.

2.8 Least Squares Adjustment

When a geodetic network is created, additional redundancy in the measurement setup is needed so as potential errors to be detected and the network's reliability to be improved. These extra measurements create a situation where there is not just one perfect solution that fits all the network conditions precisely. To handle this, a method is needed to adjust the measurements so they meet the required conditions. These corrections are known as observation residuals. The least squares adjustment method is used to adjust the measurements by minimizing the sum of the squares of these residuals. This helps ensure that the adjusted measurements fit the network model as closely as possible (Tiberius et al., 2022 & Sweco Nederland B.V., 2024).

Every least squares adjustment process is divided in two equally critical models, the mathematical and the stochastic (Tiberius et al., 2022 & Sweco Nederland B.V., 2024):

- The mathematical model refers to the Equations that describe the relationships between the observations (measurements taken) and the unknowns (coordinates of stations in a network). For instance, in a 1D leveling problem, the relationship is linear:

$$Dh_{ij} = h_j - h_i. \tag{2.6}$$

The approximation of values is essential, since it refers to the initial guesses for the unknowns, and poor guesses can cause non-convergence. Additionally, nuisance parameters are extra unknowns not directly related to the primary goal, such as transformation parameters, scale factors, refraction coefficients, azimuth offsets and orientation unknowns. Deciding whether to fix or estimate these parameters requires careful consideration to avoid overconstraining or overparameterization.

Scale factors are essential for fine-shaping the model in *MOVE3*. Typically, one scale factor is sufficient, although up to 10 can be used. They help correct biases in measurement equipment and prevent overconstraining the network. A free scale factor adjusts the network to fit known stations, but it can sometimes mask outliers, making them undetectable. It is recommended to check the scale factor value after adjustment and rerun it with a fixed scale if necessary.

- Geodetic observations are treated as random variables within the stochastic model, acknowledging measurement uncertainty. For example, if an individual measures the distance between two points multiple times, each measurement will yield slightly different values due to variations in precision and potential measurement errors. This implies that, besides the mathematical model, it is essential to develop a second model that accounts for the random variations in the observations; this is known as the stochastic model.

  Often it can be assumed that these variables follow a normal distribution characterized by a mean (μ) and a standard deviation (σ). The mean represents the expected value, while the standard deviation indicates precision. The probability distribution determines the likelihood of observation values falling within certain ranges.

  Two or more observables can be interdependent or correlated, meaning that a change in one observable will affect the other. This correlation between two observables, y_1 and y_2, is mathematically represented by the covariance $\sigma_{y_1 y_2}$. The covariance is also used to calculate the correlation coefficient, defined as

$$\rho = \frac{\sigma_{y_1 y_2}}{\sigma_{y_1} \sigma_{y_2}} \tag{2.7}$$

  The correlation coefficient ranges from -1 to 1. In case the observables are not interdependent, ρ equals 0.

  In practical terms, standard deviations are based on field conditions, instrument type, and experience. They are divided into absolute and relative parts, accounting for the dependence on the distance between stations. The variance-covariance matrix Q_y includes the standard deviations of observables, influencing the precision of the adjusted unknowns.

Statistical Testing

The purpose of statistical testing is to determine if the mathematical and stochastic models used accurately reflect reality. Additionally, potential outliers in the data need to be identified, as these can significantly affect the accuracy of the results. Therefore, statistical testing is vital for quality control. The testing in *MOVE3*, performed alongside least squares adjustment and based on the analysis of least squares residuals, includes three statistical tests: the F-test, W-test, and T-test.(Sweco Nederland B.V., 2024 & Tiberius et al., 2022).

- **F-test:** The *F-test* is a common statistical test used to check the null hypothesis (H_0) in multi-dimensional models, providing an overall model test. It tests whether the model is a good fit for the data.

  Rejection of H_0 can stem from gross errors, incorrect mathematical models, or overly optimistic a-priori variance estimates. If H_0 is rejected, further investigation is necessary to identify the cause, such as using the *W-test* for potential gross errors in individual observations. The *W-test* and *F-test* are related through a common power value (γ) in the B-method of testing (Baarda, 1968).

  To address model inaccuracies, improvements must be made to the mathematical model. Additionally, adjusting the standard deviations of observations can remedy issues with the variance-covariance matrix. Ultimately, statistical testing aims to detect outliers and model errors rather than simply accepting all observations.

- **W-test:** The *W-test* (also known as data-snooping) checks for outliers (gross errors) in individual observations, assuming one observation is erroneous while the others are correct.

  The *W-test* statistic is computed by dividing the least-squares residual by its standard deviation. This statistic helps to assess whether a particular observation is an outlier. Specifically, if the value significantly deviates from zero, this suggests that the observation may contain a gross error, assuming the covariance matrix is diagonal and the residuals are normally distributed with zero mean.

  To apply this test in practise, one must compute the residuals for each observation. If the *W-test* statistic for a specific observation is large in magnitude, it provides evidence of a potential outlier. Thus, this test is particularly useful in situations where we assume that only a single observation might be erroneous while the rest of the data points are accurate.

  In cases where the covariance matrix is not diagonal, the W-test may need adjustments or alternative methods for detecting outliers, as the assumption of uncorrelated errors no longer holds.

- **T-test:** The *T-test* is used for multi-dimensional observations, like GNSS/GPS baselines, where testing individual components (e.g. DX, DY, DZ) separately is insufficient. It is effective for identifying outliers in known stations, where traditional data-snooping may fail to detect subtle deformations that impact multiple coordinates.

Precision & Absolute Ellipses

In the context of *MOVE3*, absolute standard ellipses represent the precision of station positions within a geodetic network by illustrating the propagation of random errors through the adjustment model. These ellipses, defined by semi-major and semi-minor axes and their orientation relative to the coordinate system, indicate the spatial uncertainty of each station's position. A standard absolute ellipse typically corresponds to a 39% confidence level, while a 95% confidence level requires scaling the ellipse by a factor of 2.5 (Sweco Nederland B.V., 2024). The interpretation of these ellipses can be challenging due to their dependency on the choice of base stations, as different base stations can alter the magnitude and orientation of the ellipses, affecting the assessment of network precision.

2.9 Dilution of Precision (DOP)

DOP is a term used in satellite navigation and geolocation to describe the geometric strength of the satellite configuration on the accuracy of the position fix. It is a measure of how the satellite geometry impacts the precision of the position estimates. A lower DOP value indicates a better satellite geometry and, therefore, a more accurate position fix. Conversely, a higher DOP value suggests poorer satellite geometry, leading to less accurate position estimates (Yuen, 2009 & Langley, 1999).

There are several types of DOP, including:

- Horizontal Dilution of Precision (HDOP): Satellite's geometry effect on the horizontal position accuracy (latitude and longitude).
- Vertical Dilution of Precision (VDOP): Satellite's geometry effect on the vertical position accuracy (altitude).
- PDOP: This is a combination of HDOP and VDOP, reflecting the overall effect of satellite geometry on 3D position accuracy.
- Time Dilution of Precision (TDOP): This reflects the effect of satellite geometry on the accuracy of the timing information.

The concept of DOP can be adapted for use in the context of 5G network antennas. It can evaluate the positional accuracy influenced by the geometry of 5G antennas in a given area.

2.10 Performance Metrics

The metrics that can be obtained through the utilization of the Quectel RM520n-GL, the 5G modem, and can significantly contribute to the outcomes of this project are RSSI, RSRQ, RSRP and Signal to Interference Noise Ratio (SINR). According to Afroz et al., 2015:

- **RSSI**: This measures the total power of the signal received by the user device across the entire frequency band. It includes main signals, co-channel non-serving signals, and even noise. This measurement, expressed in dBm, is vital for assessing the overall signal strength.
- **RSRQ**: It is a cell-specific metric that indicates the quality of the received reference signal. It helps differentiate between cells based on signal quality, complementing RSRP measurements. This metric is essential for tasks like cell reselection and handover decisions. Mathematically, RSRQ = RSRP / RSSI. A higher RSRQ value means better quality, as this leads to the conclusion that the received reference signal is stronger in comparison to the overall received signal strength.
- **RSRP**: It measures the average power of the signal received from the base station. It's crucial for various functions like determining the best cell for a user device, managing handovers, and ensuring stable connections. RSRP values are measured in dBm, and if they are too low, it could indicate an unstable or nonexistent connection.
- **SINR**: It indicates the quality of the received signal by comparing its power to the sum of interference and noise. It is measured in dB and is particularly useful at the user device level for determining throughput values based on radio conditions.

The assessment of the metrics RSRQ and RSRP depends on the Figures 2.9 and 2.10

RSRQ	Signal quality	Description
0 dB to -10 dB	Excellent	Strong signal. Data speed will not be limited by the radio connection - other factors (such as congestion or throttling by your mobile provider) will affect performance. Improving the signal strength further will not improve speed.
-10 dB to -15 dB	Good	Strong signal. Improving the signal strength further (or reducing interference) will produce only small speed improvements.
-15 dB to -20 dB	Fair to poor	The connection is likely to be reliable, but slow. Drop-outs are possible. Improving the signal strength (or reducing interference) should produce a good improvement in speed.
-20 dB to -30 dB	No signal - interference too strong	Disconnection

Figure 2.9: Relationship between RSRQ and signal quality, where signal quality degrades as RSRQ values decrease.

RSRP	Signal strength	Description
-60dBm to -80dBm	Excellent	Strong signal. Data speed will not be limited by the radio connection - other factors (such as congestion or throttling by your mobile provider) will affect performance. Improving the signal strength further will not improve speed.
-80dBm to -90dBm	Good	Strong signal. Improving the signal strength further will produce only small speed improvements.
-90dBm to -100dBm	Fair to poor	The connection is likely to be reliable, but slow. Drop-outs are possible. Improving the signal strength should produce a good improvement in speed.
-100dBm to -120dBm	No signal	Disnonnection

Figure 2.10: Relationship between RSRP values, demonstrating that higher RSRP (closer to 0) correlates with stronger signal and better data speed.

2.11 Studies and Approaches employed in Related Research

Shang et al., 2014 explored RSSI based location techniques in wireless sensor networks, emphasizing accurate RSSI reception critical for precise positioning. The research analysed RSSI distribution trends, established a signal propagation loss model, and used Gaussian fitting to determine a relationship between RSSI and distances, complemented by linear interpolation for any RSSI based distance calculation. The study also introduced a new positioning algorithm, selecting anchor nodes via RSSI vector similarity degree and employing a quadrilateral location unit for enhanced accuracy. Utilizing these two mechanisms and the generalized inverse method for coordinate determination, the algorithm demonstrated a location error of approximately 17.6% in simulation experiments (Shang et al., 2014),

The RSSI positioning technique using trilateration and multilateration, is also examined by Ismail et al., 2019. More specifically, wireless sensor module used in this research operates

with long-range radio at a frequency of 868 MHz. In this study, trilateration uses three received nodes, while multilateration uses four. The transmitted node was positioned at 32 different locations within a 10x10 meter outdoor area. Results indicated that the error for multilateration is 1.83 meters, compared to 2.30 meters for trilateration. Although, the maximum and minimum errors for multilateration ranged from 1.00 to 5.28 meters, and for trilateration, they ranged from 0.5 to 3.61 meters, the study concluded that multilateration offers greater accuracy than trilateration, and increasing the number of received nodes improves the localization accuracy of the transmitted node (Ismail et al., 2019).

Carl Rydholm and William Pommer tried to estimate the position of the user equipment following a comprehensive simulation of GNSS and 5G systems (Rydholm and Pommer, 2021). They simulated GNSS pseudo-range measurements by calculating satellite positions, filtering out satellites below a 15°elevation angle, and adding realistic clock offsets and Gaussian noise. Pseudo-range errors were considered with fixed values to account for receiver inaccuracies. For 5G they considered measurements of AOD and RTT. AOD measurements were refined using interpolation and were based on signal strength from different base station sectors, while RTT measurements were derived from the time a signal took to travel to and from the base station. The hybrid positioning solution integrated these measurements using a weight least squares approach combined with the Gauss-Newton method to optimize position estimates, accounting for measurement error sand sector-specific performance.

The methodology used by Pileggi et al., 2023 involves deploying eleven custom-built 5G base stations in a test area covering various environments (indoor, outdoor open sky, and obstructed outdoor areas). A trolley equipped with a 5G receiver and data storage unit collected ToA measurements while following predefined trajectories. These trajectories were accurately benchmarked using a total station. The collected ToA data were processed using the least squares method to minimize errors and optimize position estimation. Various multilateration techniques were also tested, using ToA measurements from multiple base stations to determine positions by intersecting distance spheres. Additionally, hybrid positioning algorithms that combine 5G ToA data with GNSS were explored to leverage the strengths of both systems. The study also implemented error mitigation techniques like filtering, smoothing, and outlier detection to refine the data. These strategies were compared across different environments, showing positional accuracies ranging from decimeters to a few meters, thus demonstrating the potential of 5G ToA measurements to enhance positioning accuracy where traditional GNSS systems are limited (Pileggi et al., 2023). Figure 2.11 illustrates the distribution of the eleven 5G transmitting reference points and the equipped trolley used for acquiring 5G signals along predefined trajectories in both indoor and outdoor areas.

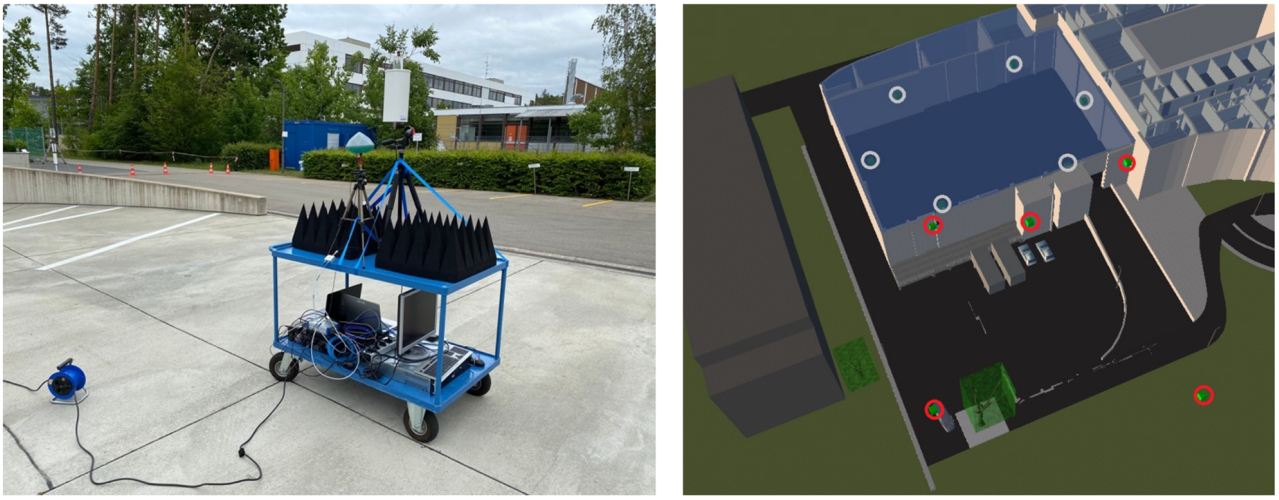

Figure 2.11: Distribution of eleven 5G transmitting reference points and the equipped trolley used for acquiring 5G signals along predefined trajectories in both indoor and outdoor areas (Pileggi et al., 2023).

Alghisi and Biagi investigated how integrating 5G with GNSS can enhance positioning accuracy in urban settings with limited satellite visibility. Using simulations, They evaluated GNSS satellite visibility and PDOP across different urban scenarios. The study found that while satellite visibility and PDOP are generally better in residential streets, urban canyons pose significant challenges. The paper also explored the potential of combining 5G base station data, specifically ToA and TDoA measurements, with GNSS data. In conclusion, optimal 5G configurations can significantly improve positioning accuracy in urban canyons, with five base stations resolving positioning issues entirely, while fewer stations provide partial improvements (Alghisi and Biagi, 2023).

Chapter 3

Methodology

3.1 Selection of Positioning Method

RSSI-based 5G positioning over the more advanced methods such as TDoA, AOA, and MC-RTT offers several practical advantages.

First of all, RSSI-based positioning only requires measuring the signal strength received by the user's device from three or more base stations. No complex hardware like synchronized clocks or antenna arrays are needed, making it easier to implement and deploy. By contrast, TDoA and MC-RTT demand precise synchronization between multiple base stations and the user's device. AOA and AOA require advanced antenna arrays and beamforming technologies, which may not be available in all 5G deployments. Implementing these methods requires additional hardware both at the base stations and possibly on the user's device, complicating deployment and increasing costs.

TDoA, AOA, and MC-RTT positioning methods can offer superior accuracy, and they are designed for use cases where extreme precision is necessary, like autonomous driving or industrial automation. For more general applications like outdoor positioning, indoor navigation or asset tracking, positioning via RSSI may provide sufficient accuracy at a fraction of the cost and complexity.

Furthermore, the more advanced positioning techniques, rely on proprietary features of specific 5G vendors. Different equipment manufacturers might implement these techniques in slightly different ways, leading to incompatibilities in real-world scenarios. On the other hand, RSSI is a universal metric that is not vendor-specific. It is measured consistently across devices and networks, making it a more widely applicable and neutral choice for research.

3.2 Proposed Methodological Approach for Data Collection and Position Estimation

The first phase of the methodology includes static measurements and analysis of the RSSI values that are transmitted from a specific antenna. Starting statically isolates the RSSI variation over time in a stable environment. This is essential for understanding the natural fluctuations in signal strength without the influence of mobility or environmental factors. It allows the establishment of a baseline for how reliable RSSI is a metric for distance calculation. Skipping this phase or introducing moving or environmental complexity too early would obscure the fundamental behaviour of RSSI. More complex setups, like testing with

multiple base stations right away, would introduce too many variables at once, making it harder to identify how much of the error is due to RSSI variability versus other factors.

Antennas play a critical role in signal reception, and testing multiple antennas can help exploring how hardware configurations impact RSSI measurements and the overall accuracy of positioning. By testing the different antennas' effects, the most suitable configurations for reliable 5G positioning can be identified. Optimizing the hardware setup and ensuring that the findings are not hardware-dependent can make the research more widely applicable. The reliance on one single antenna type can lead to limited understanding of how different antenna characteristics (e.g. gain, type) affect performance.

The FSPL Equation assumes ideal LOS conditions, so testing it in such an environment allows the validation whether the theoretical model accurately predicts distance. This is a critical step in ensuring that the model works before applying it to more complex conditions. The earlier introduction of non-LOS environments would complicate the analysis since the signal propagation parameters such as multipath effects or interference would be faced in an early stage. By first testing in LOS conditions from specific cell tower again, the FSPL Equation is validated in its intended use case, providing a solid foundation for further experimentation. In this case, the GNSS-RTK is also used so the user their location.

In the second phase of the methodology, multiple cell towers' signals are used to calculate the distances between the user's device and the towers based on the FSPL model, which translates RSSI values into distance estimates. This trilateration approach enhances accuracy, especially in 5G environments with dense tower deployments. The method leverages *MOVE3* software for least squares adjustment, which refines these distance estimates by minimizing the error between observed and actual values, improving positioning accuracy. The use of this technique is particularly effective because it accounts for signal variability and ensures that the results are more reliable than using raw RSSI data alone. By comparing the refined estimates to the real position obtained from a GNSS-RTK device, this method validates its efficacy for 5G positioning in real-world conditions.

3.2.1 Data Acquisition

Data acquisition depends on the two devices that are presented in Appendix A, the modem and the GNSS-RTK device. Both devices were set up by Ericsson on a laptop running the Linux operating system.

The modem is used to retrieve information about the transmitted signal of every cell tower that is operating in the *Vodafone* network. A Subscriber Identity Module (SIM) card is attached to it for this reason, and the command-line tool *qmicli* is utilized. The latest is part of the *Libqmi* project, a Linux library to control Qualcomm MSM Interface (QMI) devices, which are commonly used in mobile broadband modems. The *qmicli* tool allows users to interact with QMI devices by sending QMI protocol commands directly to the modem and receiving responses. The commands that were used in this research were (Steffens, 2023):

- *nas-get-cell-location-info*: this command retrieves information about the cell towers to which the modem is currently connected. The output typically includes information like PCI, Location Area Code, Tracking Area Code, Mobile Network Code. Apart from those, it also gives information about the RSSI, RSRQ and RSRP values which are then used for the implementation of the trilateration method. The output is demonstrated in Figure 3.1.

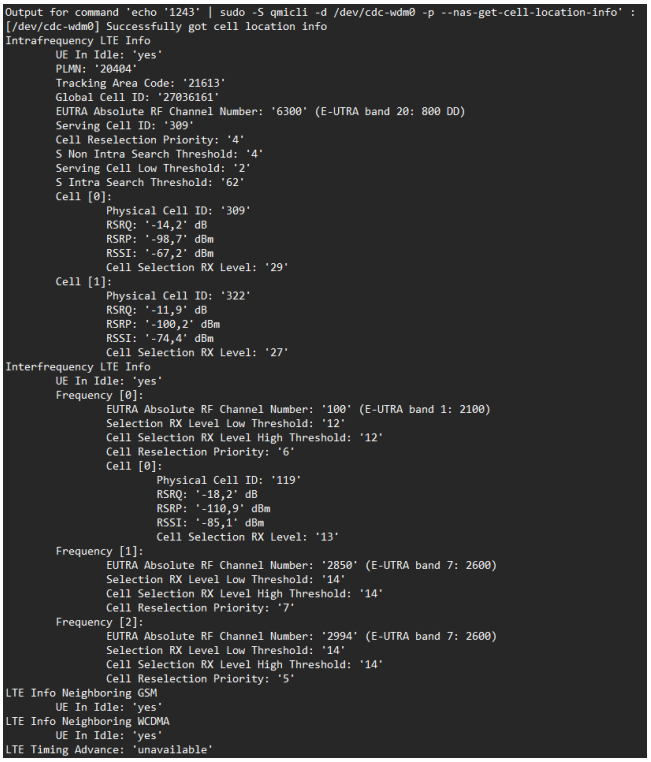

Figure 3.1: Cell tower location information of the received signal — *nas-get-cell-location-info* command output example.

- *nas-get-signal-info*: this Command provides Detailed Signal Information, including Metrics such as RSSI, RSRQ and SINR, not for each Individual PCI, but considering all the Available Neighboring Cell Towers. The output is demonstrated in Figure 3.2.

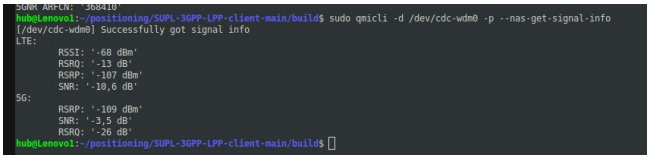

Figure 3.2: 5G signal information — *nas-get-signal-info* command (output example).

Before implementing the trilateration method in order to identify the position of the user's equipment in space, the distances between the observation point and the cell towers of the network need to be defined as described in Section 3.2.2. In order to achieve this, the association of the PCI of each antenna that is displayed in the output of the *nas-get-cell-location-info* with the corresponding information from the *Excel* file containing the data about each antenna (see Section A.4) was necessary. In the end, the user is able to extract the coordinates of all the antennas that the modem is receiving signal from.

The u-blox C099-F9P GNSS-RTK device offers the potential for centimeter-level accuracy through RTK corrections. However, achieving this precision depends on the accuracy with which the base station's reference point is measured. The device can request assistance data from a location server to enhance positioning speed and reliability. Since this project's focus is outdoor positioning, this device is used to extract the coordinates of the user's equipment so as the distance to the cell towers is calculated. Initially, extracted data was utilized to determine the distance from a specific cell tower and evaluate signal propagation based on

that distance. Eventually, it transitioned to validating the actual position against the position calculated using RSSI values from the 5G network.

An example client is used by *Ericsson* that requests data from a location server. It supports multiple requests such as OSR, SSR and Augmented GNSS (AGNSS). The program takes an interface and port associated with the *U-blox* receiver as arguments. Then it is connected, configures the device to output *UBX-NAV-PVT* which are parsing messages that provide position, velocity, and time data. Finally, all received messages are printed to *stdout*. In the output latitude and longitude are represented by *lat* and *lon* respectively. The horizontal 1-sigma accuracy is indicated by *h_acc*. An example is shown in Figure 3.3.

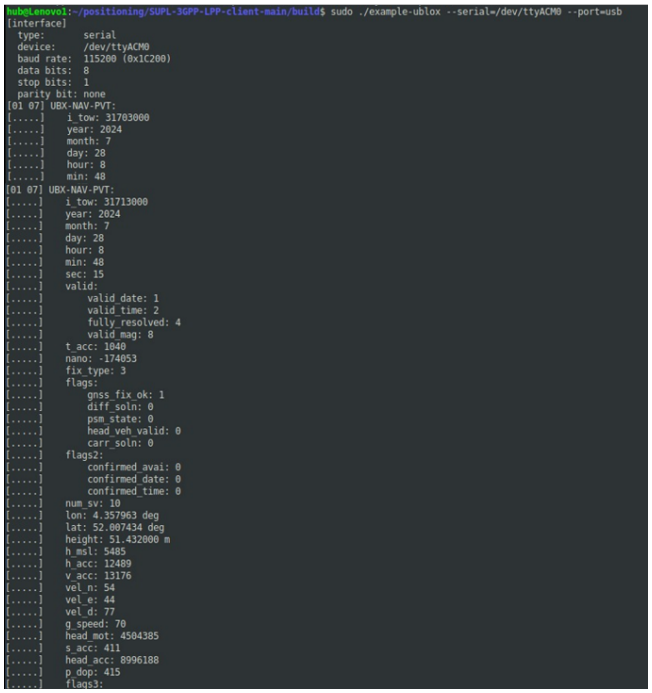

Figure 3.3: Output information of the GNSS-RTK device.

- Static Measurements

  The initial approach was the collection of data when the devices were both in a fixed position throughout the measurement period. This method enabled a thorough analysis of signal propagation characteristics in a controlled environment helped to mitigate transient fluctuations through averaging. It served as an essential first step in ensuring the reliability of the collected data and validating the signal's stability over time at a known location before extrapolating the model to dynamic scenarios.

- Multiple Antennas Testing

  The incorporation of different types of antennas took place, so as the signal behavior could be evaluated in terms of consistency and reliability. A deeper understanding of the impact of antenna properties on signal strength and distance calculations was developed and insights were gained into how different antennas affect signal propagation characteristics.

- FSPL test along a direct LOS of a specific transmitter

  Conducting a FSPL test was an essential step in understanding how signal strength diminishes over distance. Of course, a real environment consists of multiple obstructions that affect the signal. However, the paths that were selected for this step were the ones

where there was as much as possible clear line of sight between the cell tower and the modem. This step of the research project contributed in comparing real-world measurements to the theoretical model in order loss factors to be better understood, and the theoretical predictions to be compared with real data.

The tests were conducted using two distinct approaches. Initially, measurements were systematically taken at fixed intervals from the antenna, starting at 50 meters and increasing in increments of 50 meters. This approach allowed for the observation of how signal strength diminishes as distance from the antenna increases. By spacing measurements at regular intervals, a clear pattern of signal attenuation over distance could be established, essential for understanding the effective range and coverage area of the antenna.

Continuous measurements were also conducted to provide a more granular and detailed spatial analysis. Unlike the interval approach, which provides data points at specific distances, continuous measurements offer a comprehensive view of signal variation across the entire area under study. This method captures nuanced variations in signal strength due to factors such as terrain, obstacles, and environmental conditions, providing a richer dataset for further analysis and modeling.

The most important conclusion of this step was the identification of the obstructions that affect the signal in a real environment. The data collected were firstly analyzed with plots or diagrams that show the fluctuation and overall behavior of the signal over distance. Information was obtained regarding the antenna's effective range too.

The second part of the step included the visualization of the measurements in a 3D map created with *QGIS* and the plugin *qgis2threejs*. Having already created plots and diagrams for the signal propagation, a spatial analysis could be performed so as patterns, trends and anomalies of it could be identified. A more intuitive and comprehensive view of the data was produced that facilitated easier identification of areas with strong and weak signal coverage.

The 3D maps were created using datasets from AHN4 and 3DBAG. Initially, the building datasets from 3DBAG were obtained from their website as a geopackage file containing comprehensive data for all buildings in the Netherlands. Subsequently, AHN4 LiDAR point clouds were downloaded from GeoTiles. These point clouds underwent classification before integration into the project in QGIS. Buildings were extracted to avoid overlap with those from 3DBAG, while ground points were removed to optimize file size and facilitate faster analysis. Following this, antenna data was imported as a delimited text file containing coordinates for both antennas and observation points, along with corresponding RSSI values. These values were then visually enhanced through gradual colorization based on their respective RSSI values.

3.2.2 Position Estimation through Trilateration Method using *MOVE3* Software

The final step of the methodology involves the utilization of *MOVE3* software to eventually analyze the accuracy of 5G positioning via RSSI and compare it with the

'ground truth' given by the GNSS-RTK device. In the beginning, a *CSV* file is imported with cell tower coordinates and another file with the estimated distance measurements from observation points to these towers. *MOVE3* firstly approximates the positions of the observation points and then performs a least squares adjustment to refine these positions based on the observed data. Lastly, a report is extracted to evaluate the accuracy of the model, the standard deviations are adjusted so as the F-test is validated, and the precision of the network is ensured by the identification of the outliers.

More specifically, a new project is created in the *MOVE3* software, using the Rijksdriehoekscoördinaten (RD) projection, officially known as the Amersfoort / RD New coordinate system (European Petroleum Survey Group (EPSG):28992). Initially, a *CSV* file containing the coordinates of each cell tower in the *Vodafone Ziggo* network is imported. The format of this *CSV* file is *(CellTower_PCI, X East, Y North, Height)*, where the values represent the PCI of the cell tower antenna, its coordinates in the X (East) and Y (North) directions, and its height above sea level.

Next, another *CSV* file is imported into the project, which contains the measured distances from the observation points to the cell towers. It is crucial to ensure that the PCI values in both files are formatted consistently. This second CSV file is imported as "TotalStation" data, with the manufacturer specified as "MOVE3 csv". This is because the type of observation is similar: both the total station data and the RSSI data involve distances, but the total station data also includes directions (horizontal and vertical angles) while the RSSI data only includes distances. The format of this file is *(Observation, Known_CellTower_PCI, height_observation_point, height_CellTower, hor_angle, ver_angle, distance)*. The values of this file represent the name of the observation point, the PCI of the cell tower antenna, the height of the observation point (not known), the height of the cell tower antenna above sea level (derived from the already imported *CSV* file), the horizontal and the vertical angle of the observation point and the cell tower antenna (also not known) and the observed distance between these respectively that is derived from the original RSSI observation.

After importing the data, *MOVE3* approximates the coordinates and displays an initial placement of the observation points on the map. The subsequent step is to force *MOVE3* to perform a least squares adjustment in the pseudo-constrained network. This process involves adjusting the positions of the observation points to minimize the sum of the squared differences between observed and calculated distances, angles, and heights. The known stations remain at their fixed positions when a pseudo-constrained network is selected.

Once the adjustment is completed, a report is exported as an XML file. This report includes the results of various tests, and it is essential to adjust the standard deviations of the observations (distances) so that the *F-test* is accepted. The *F-test* is a statistical test used to determine if the variances between two populations are equal, which is crucial for validating the adjustment (see Section 2.8).

The final step involves reading the report to identify any observations detected as possible outliers through the *W-test* results. These outliers, which do not fit well within the adjusted model, should be deselected to improve the accuracy of the network. Identifying and deselecting outliers ensures that the final model is as precise as possible, providing reliable coordinates for the observation points while the cell towers' ones

remain fixed.

STATIONS

Number of (partly) known stations	5
Number of unknown stations	1
Total	6

OBSERVATIONS

Distances	5
Known coordinates	10
Total	15

UNKNOWNS

Coordinates	12
Scale factors	1
Total	13

Degrees of freedom	2

ADJUSTMENT

Number of iterations	3
Max coord correction in last iteration	231.1319 m Tolerance exceeded

TESTING

Alfa (multi dimensional)	0.0027
Alfa 0 (one dimensional)	0.0010
Beta	0.80
Critical value W-test	3.29
Critical value T-test (3 dimensional)	4.24
Critical value T-test (2 dimensional)	5.91
Critical value F-test	5.91
F-test	2.740 Accepted

Chi-Square Test (99.9%)	
Lower Bound	0.001
Upper Bound	7.601
Chi-Square Test	2.740 Passed

Figure 3.4: Example of Results of the Statistical Testing after the Adjustment using *MOVE3* Software.

Chapter 4

Results

As already mentioned, this study investigates the effectiveness of the trilateration method for positioning based solely on the RSSI from the 5G *Vodafone Ziggo* network. The primary research question addresses the extent to which this approach can accurately determine the position of the user compared to the 'ground truth' given by the GNSS-RTK device.

This chapter presents the results of the conducted experiments and analyses following the methodological framework described in Section 3.2, highlighting the capabilities and limitations of RSSI-based positioning. In particular, the Section 4.1 reveals that the RSSI is significantly influenced by several factors. Static measurements taken with different antenna types show notable variability in RSSI values with substantial standard deviations indicating inconsistent signal strength. Initial attempts to model FSPL face challenges due to these unpredictable RSSI fluctuations. Further static measurements and trilateration performed with the *MOVE3* software demonstrate considerable positional uncertainty, with discrepancies of hundreds of meters between calculated and actual observation positions. This uncertainty is confirmed in Section 4.2 where results from the experiments depict that topographic factors, such as trees and buildings, obstruct signal propagation and cause significant variations in RSSI. Additionally, the distribution of 5G network towers affects positioning accuracy, with sparse networks leading to less reliable trilateration results as described in Section 4.3. Despite these challenges, closer proximity to cell towers improves distance accuracy, underscoring the need for denser network deployment and advanced modeling techniques to enhance position precision.

4.1 Accuracy

The subquestion regarding the potential accuracy of standalone 5G using the trilateration method to in comparison to the 'ground truth' provided by GNSS-RTK is addressed through the conducted measurements and experiments.

- **Static measurements - Multiple antennas testing**

  To evaluate accuracy, static measurements were taken using three different types of antennas were utilized to evaluate signal propagation characteristics (see Figure A.3). The initial testing site was located near Delft Central Station, as depicted in Figure 4.1. Throughout this assessment, the serving cell consistently identified was the one with PCI 486.

  The variations in RSSI were analyzed and are presented in Figures 4.2, 4.3 and 4.4 on a total of 80 measurements conducted with each type of antenna. Specifically, the first

measurement series yielded an average of RSSI of -72.09 dB, while the second series returned an average of -65.82 dB and the third series -68.93 dB. Each of these Figures illustrates significant variability in RSSI values, with corresponding standard deviations of 2.02, 2.08 and 2.55 respectively.

The variation in RSSI observed in these static measurements does not allow for a targeted selection of a single antenna type for further testing. Therefore, antennas type 3 were randomly selected for the next phase of the project.

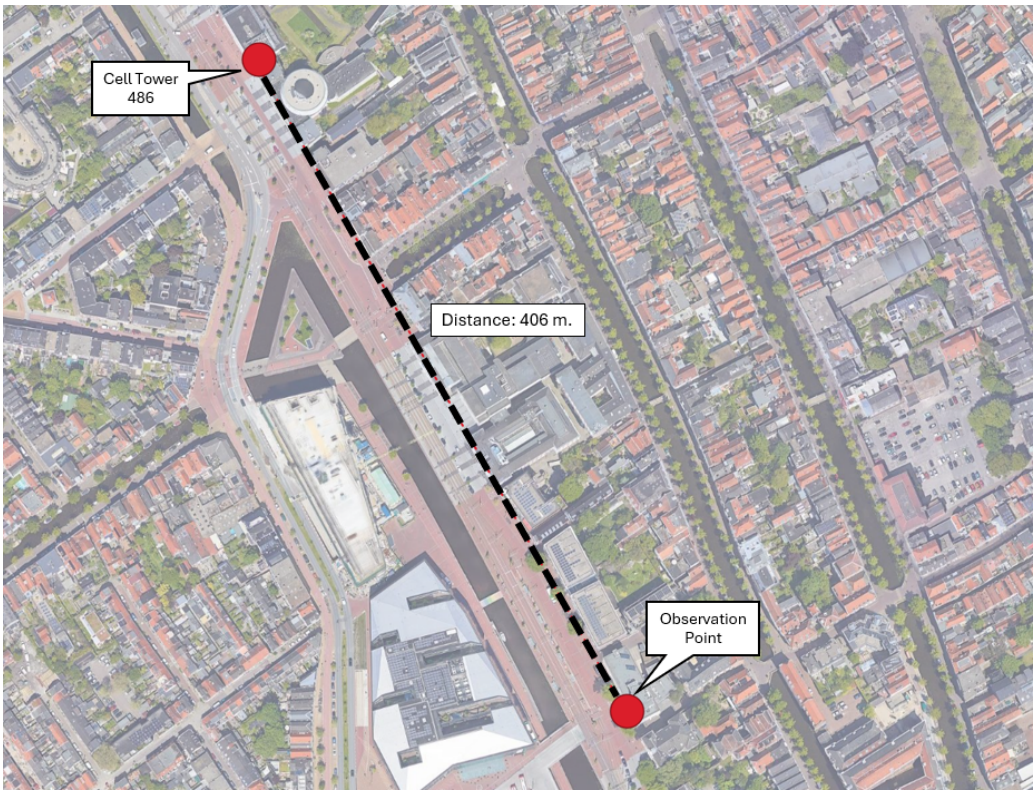

Figure 4.1: Location of observation point and serving cell 486 while statically testing the signal variation. The distance between is calculated through the GNSS-RTK device and is 406 meters.

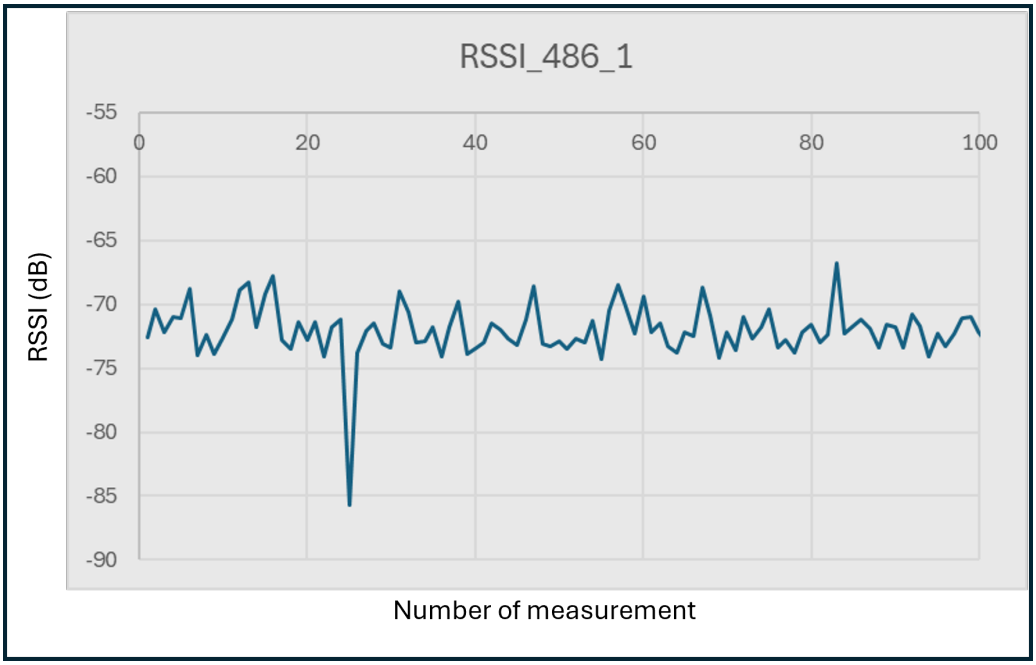

Figure 4.2: Variation of RSSI during static measurements performed with antennas type 1.

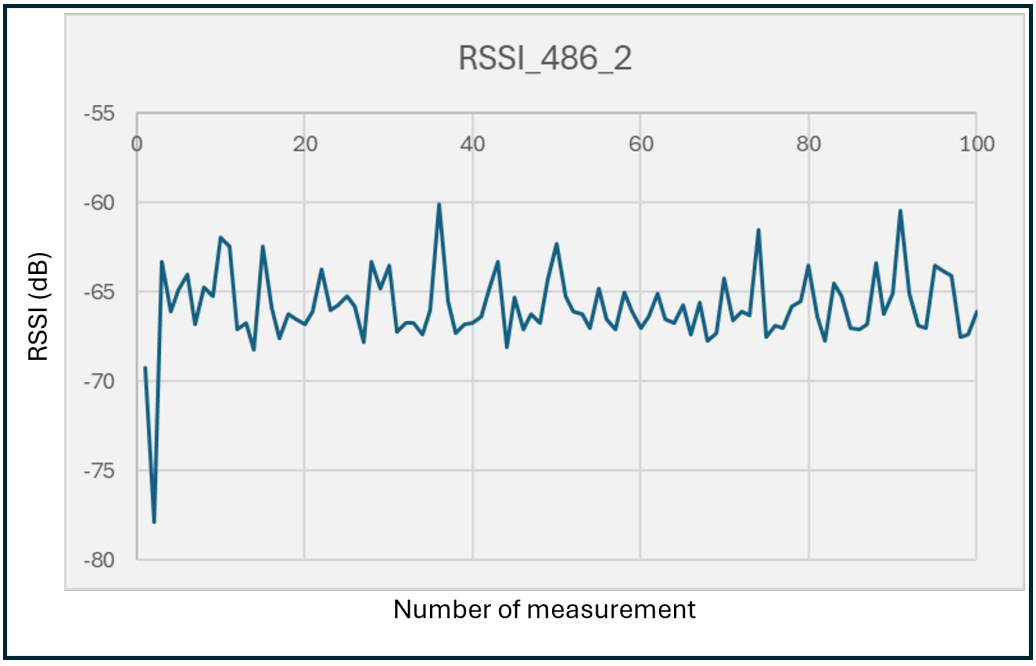

Figure 4.3: Variation of RSSI during static measurements performed with antennas type 2.

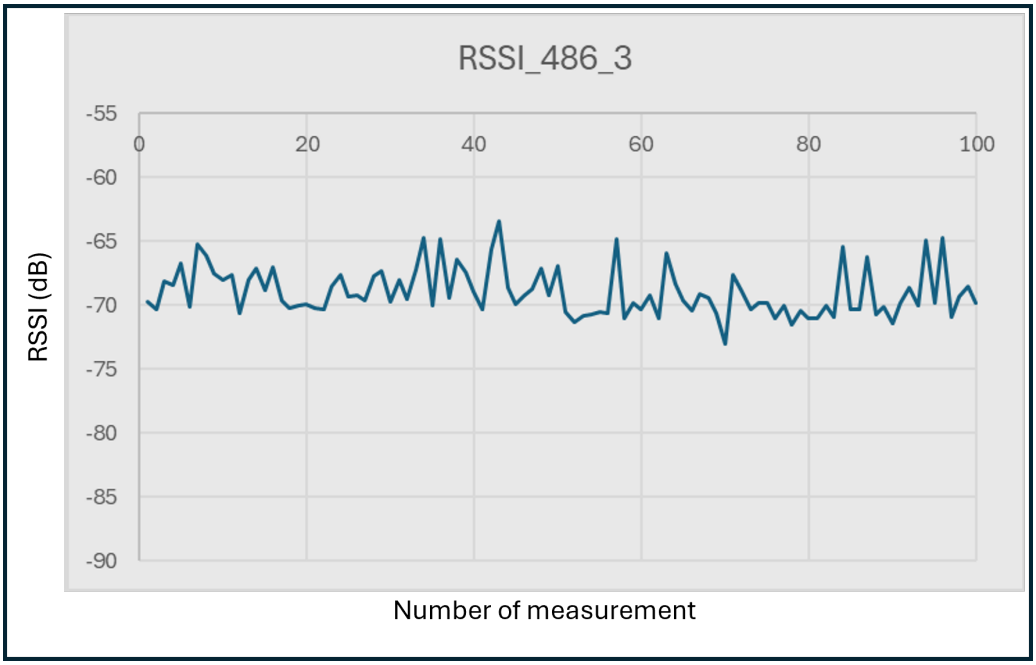

Figure 4.4: Variation of RSSI during static measurements performed with antennas type 3.

- **FSPL along a direct LOS of a specific transmitter**

  The initial attempt to test the Free Space Path Loss (FSPL) involved continuous measurements along a direct line of sight from the cell tower. In these tests, just the type 3 of the antennas was utilized (see figure A.3a).

  This approach meant that, at a very slow walking speed, the modem was concurrently measuring signal strength. The results, presented in Figures 4.5 and 4.6, exhibit significant variations in RSSI, making it difficult to derive clear conclusions or develop a reliable model for distance calculation based on RSSI.

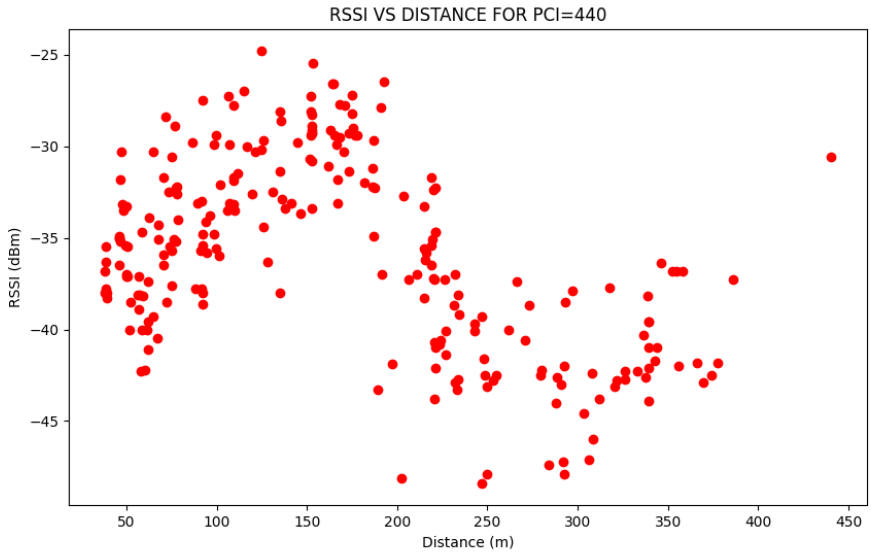

Figure 4.5: Continuous measurements of RSSI values in a direct LOS from cell tower with PCI 440.

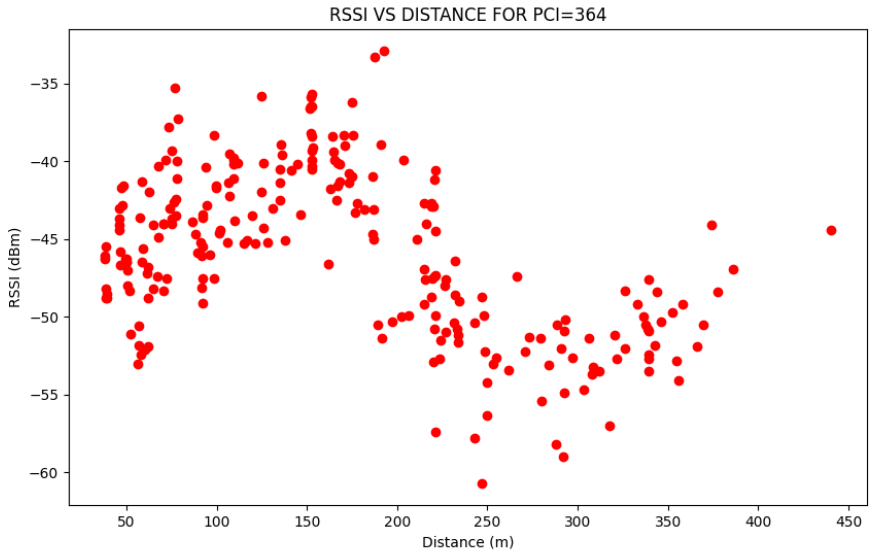

Figure 4.6: Continuous measurements of RSSI values in a direct LOS from cell tower with PCI 364.

Due to the inherent variability in RSSI values, deriving a precise model for FSPL as described in Figure 2.6 can be challenging.

Further measurements were collected at 50-meter-intervals along a straight and direct line of sight with the cell tower as depicted in in Figure 4.7, with RSSI values shown in red. While it is generally observed that RSSI decreases with increasing distance (Figure 4.8), significant variations persist. When these measurements were analyzed using a Gaussian fit, the resulting curve did not align with the expected logarithmic trend typically associated with FSPL models. This discrepancy underscores the complexities involved in accurately modeling path loss in practical scenarios, where RSSI fluctuations can deviate from theoretical predictions.

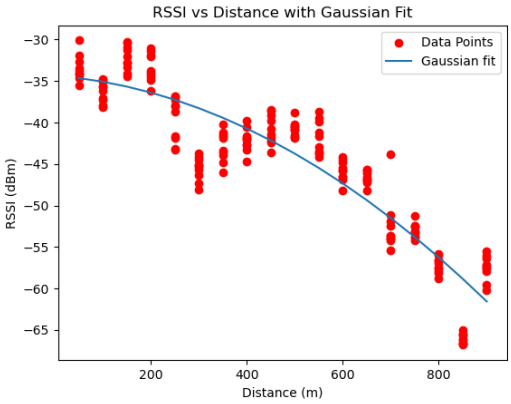

Figure 4.7: RSSI variation and Gaussian fit at 50-meter intervals (PCI 364).

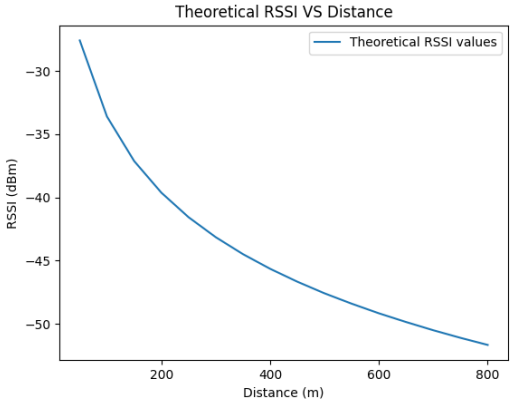

Figure 4.8: Theoretical RSSI values along distance (PCI 364).

However, measurements have demonstrated that RSSI can be highly unpredictable. For instance, as illustrated in Figure 4.9, variations are observed not only at specific distances but occasionally, the RSSI values can increase, complicating the correlation

between RSSI and distance. This unpredictability makes it challenging to infer the distance based solely on RSSI values. Such fluctuations can arise due to various factors, as detailed in Section 2.4.

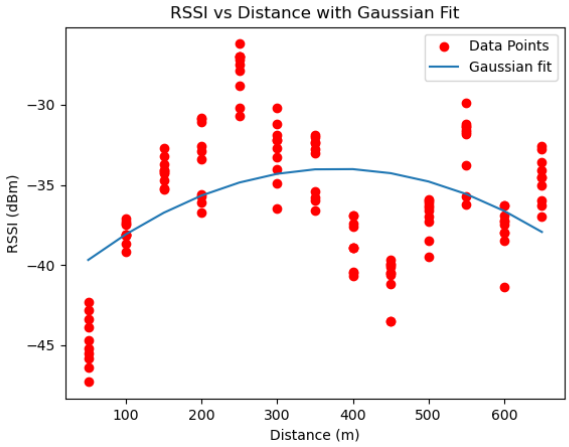

Figure 4.9: RSSI values' variation and Gaussian fit at 50-meter intervals (PCI 283).

- **Position Estimation through Trilateration Method using *MOVE3* Software**

Although the RSSI values exhibit significant unpredictability, as shown in the results above, an attempt was made to determine a position using the trilateration method. This experiment was conducted at three different locations in Delft, designated as Station, Pulse, and Park. These locations are illustrated in Figure 4.10.

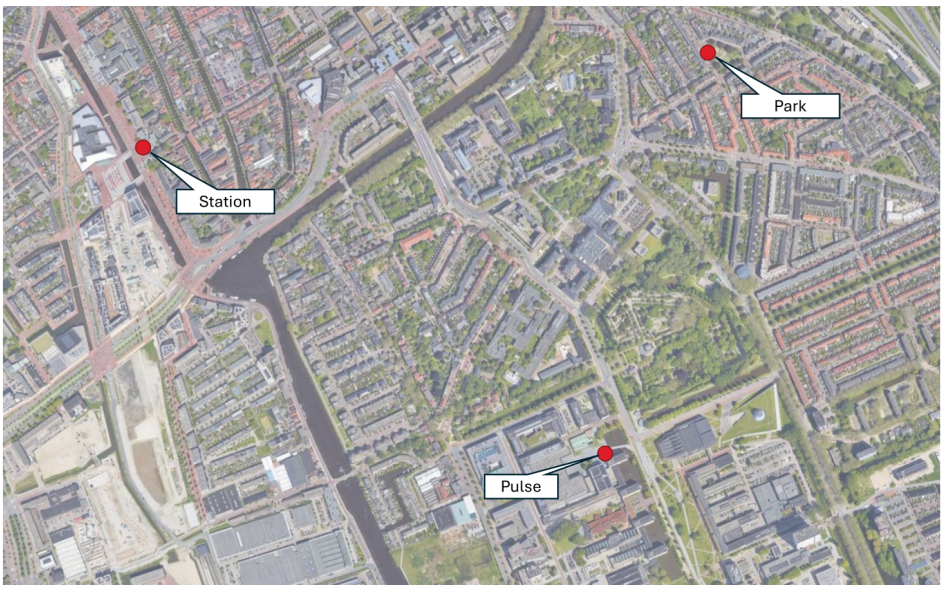

Figure 4.10: The 3 locations of the static measurements in Delft.

During the experiment, the modem remained stationary for twenty minutes at each observation point. Throughout this period, RSSI values were collected for each PCI and subsequently averaged. Using the averaged RSSI values and applying Equation 2.4, distances from the modem to the respective cell towers were calculated.

The trilateration method was applied using the *MOVE3* software to determine device's position. All calculated distances from the observation points to the cell towers were imported as total station observations, following the methodology outlined in Section 3.2.2. A standard deviation of 30 meters was assigned to each observation. Initial coordinate approximations were made, followed by the pseudo-constrained adjustment for each observation. Finally, manual data snooping was conducted to identify and reduce outliers in the observations, thereby optimizing the fit. The results are presented in Figure 4.11. The red points correspond to the observation points and the yellow ones to the calculated position of *MOVE3*.

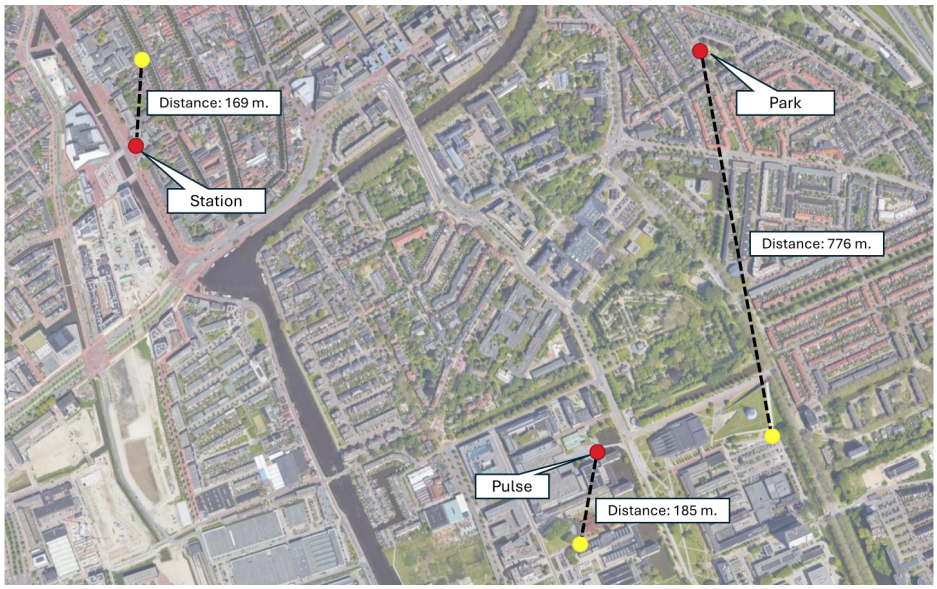

Figure 4.11: Distances between the observation points and the calculated position using *MOVE3* software.

The approximated coordinates are off by hundreds of meters from the actual observation points. This difference highlights the spatial uncertainty in the measurements. Figures 4.12, 4.13 and 4.14 show this uncertainty with ellipses around each station's position.

These ellipses represent the area of potential positional uncertainty, with their shape and orientation indicating the direction and magnitude of the most likely errors. Although the errors show a directional pattern, the large size of the ellipses signifies substantial uncertainty, indicating that while the estimates are somewhat aligned with the true positions, there is still a high level of inaccuracy.

Observation Point 1: Station

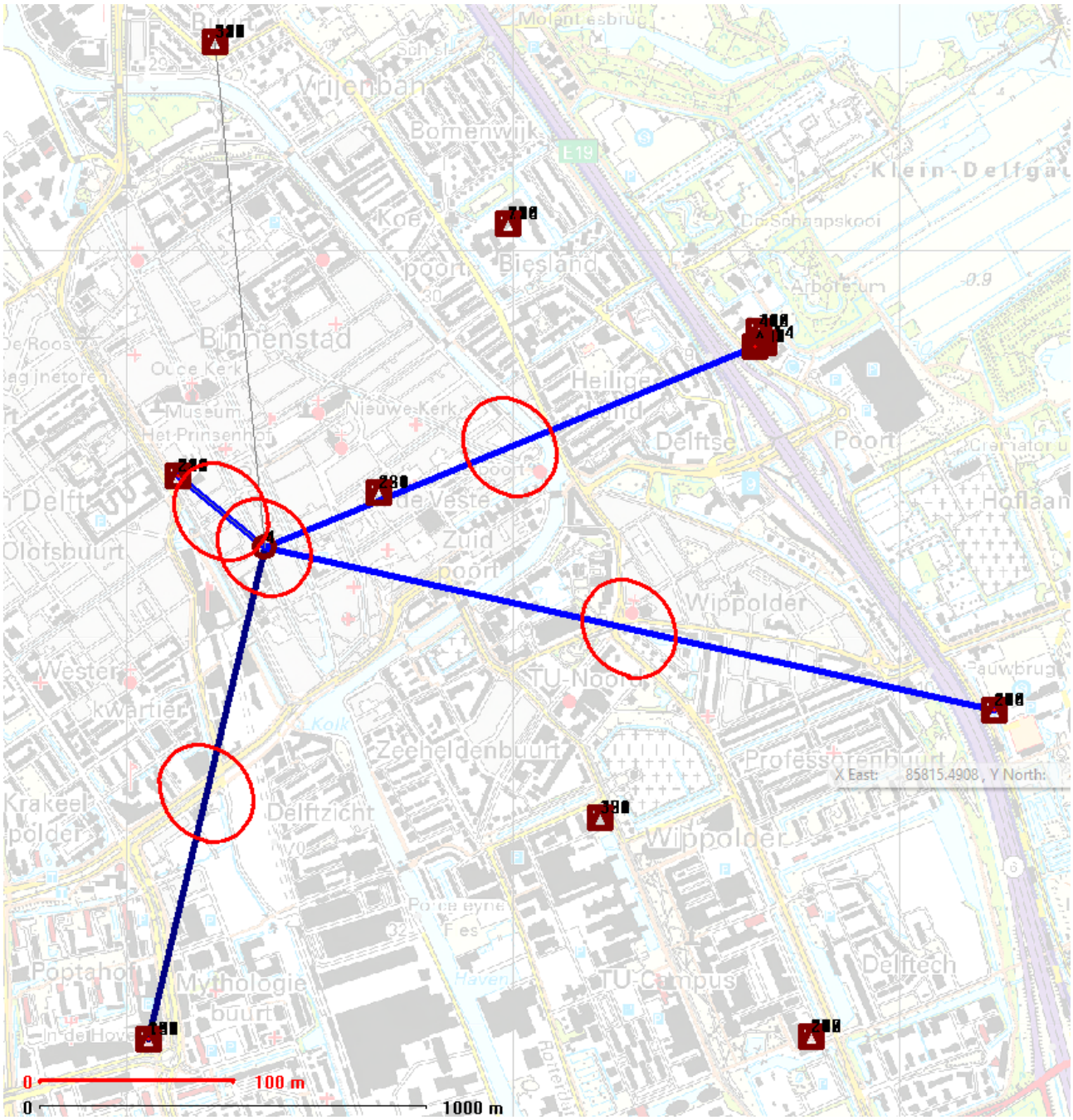

Figure 4.12: Trilateration implementation for observation point 1 using *MOVE3* software.

Observation Point 2: Pulse

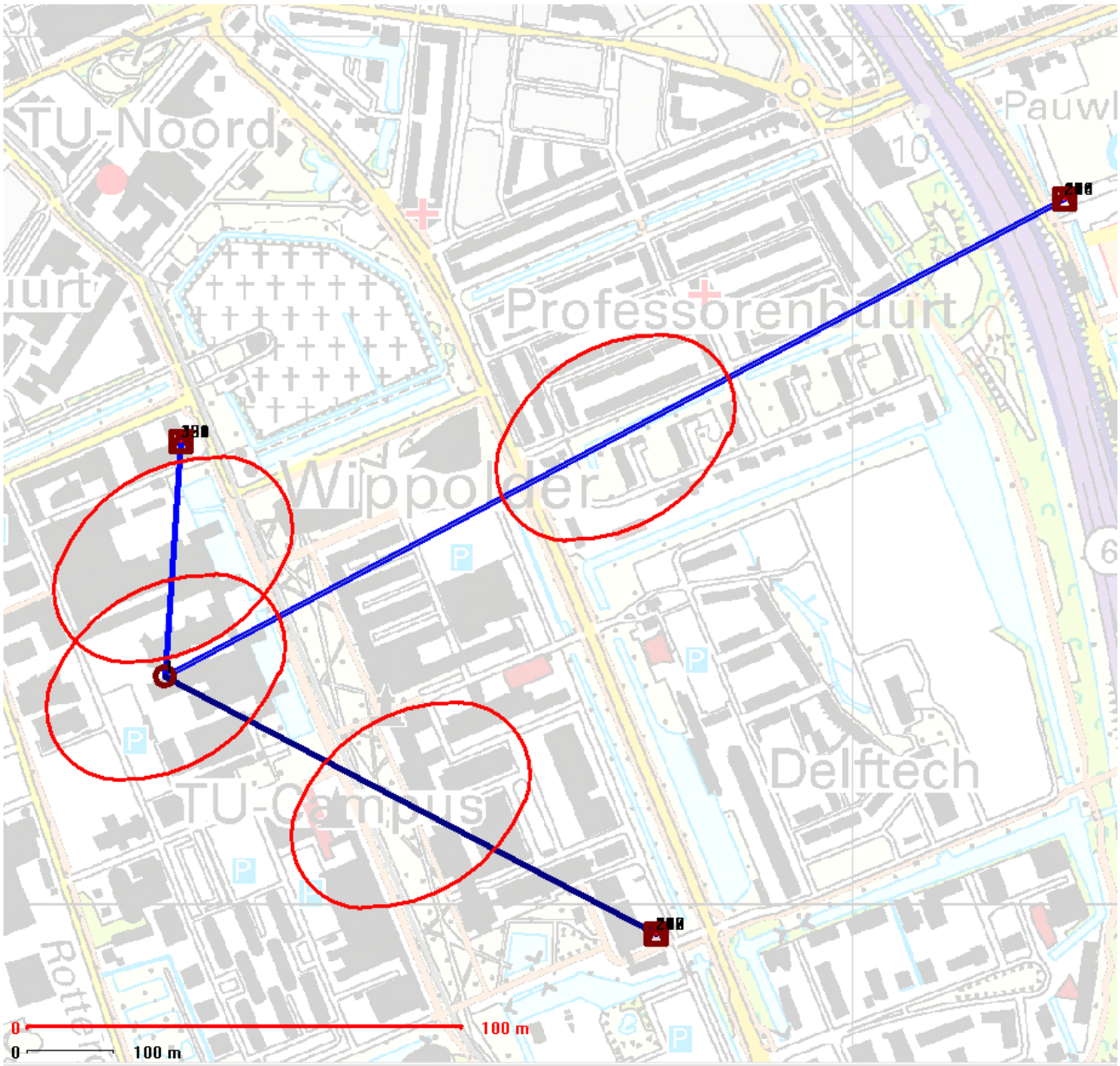

Figure 4.13: Trilateration implementation for observation point 2 using *MOVE3* software.

Observation Point 3: Park

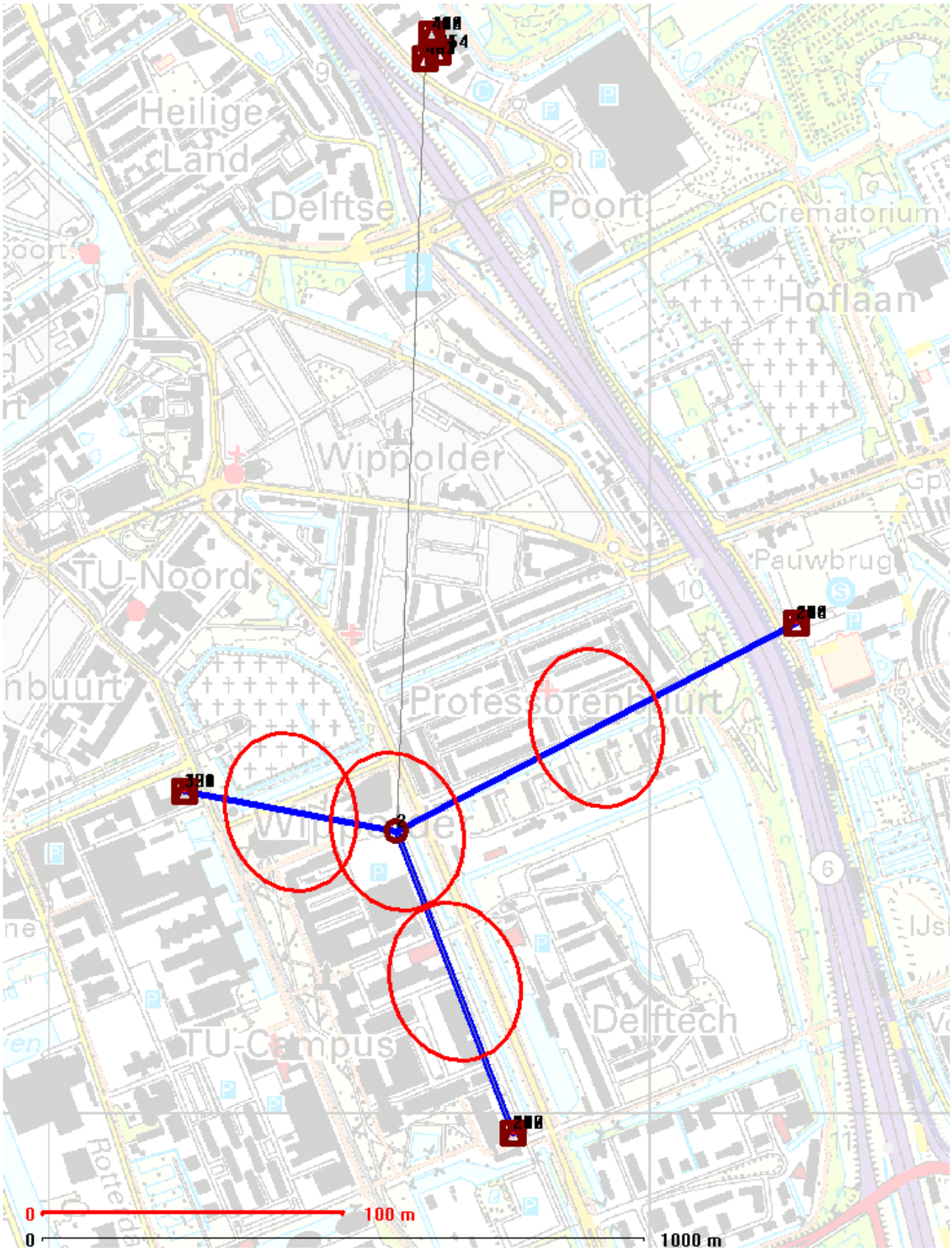

Figure 4.14: Trilateration implementation for observation point 3 using *MOVE3* software.

4.2 Impact of Topographic Factors on 5G Positioning Accuracy

Topographic factors significantly impact the accuracy of 5G positioning due to the various ways in which they can alter signal propagation as it was described in Section 2.4. These parameters may not be directly identified in a geomatics-related master thesis, but the second research subquestion "What is the impact of topographic factors (e.g. buildings, urban canyons) on the accuracy of 5G positioning" is initially answered through the following example, where 20 measurements of RSSI were taken at 50-meter intervals along a direct line of sight to a cell tower identified by PCI 208. The experiment was conducted on TU Delft's campus, specifically next to the Green Village.

The measurements were averaged and visually represented on a map, with a gradient color scheme indicating the RSSI values. Intuitively, one would expect that the RSSI would decrease as the distance from the antenna increases due to signal attenuation. However, the results did not follow this expected trend. Instead, the RSSI values varied irregularly, demonstrating higher values in certain areas despite increased distance from the antenna.

This anomaly can be attributed to the presence of trees along the path. The 3D visualization of the area corroborates this finding, showing that the highest RSSI values (indicated by the lightest color points on the map) correspond to observation points with fewer or no trees obstructing the line of sight to the antenna. Conversely, lower RSSI values (darker points) align with areas where trees are present, causing signal attenuation and scattering.

Additionally, it is notable that the first observation point in the measurements exhibits an unexpectedly lower RSSI value compared to the next few observation points. This counterintuitive result arises from the specific positioning of the cell tower and the first observation point. The cell tower is situated on the terrace of a large building, and at the same time the first observation point is close to the building, but it is positioned at ground level. Due to this placement, there is no clear line of sight from the first observation point to the cell tower, resulting in significant signal obstruction and attenuation. The building itself blocks the direct path of the signal, causing the initial RSSI value to be lower than expected despite the close distance to the tower. This case further confirms that buildings, as critical topographic factors, can drastically affect the accuracy of 5G positioning, providing another layer of evidence in response to the research subquestion.

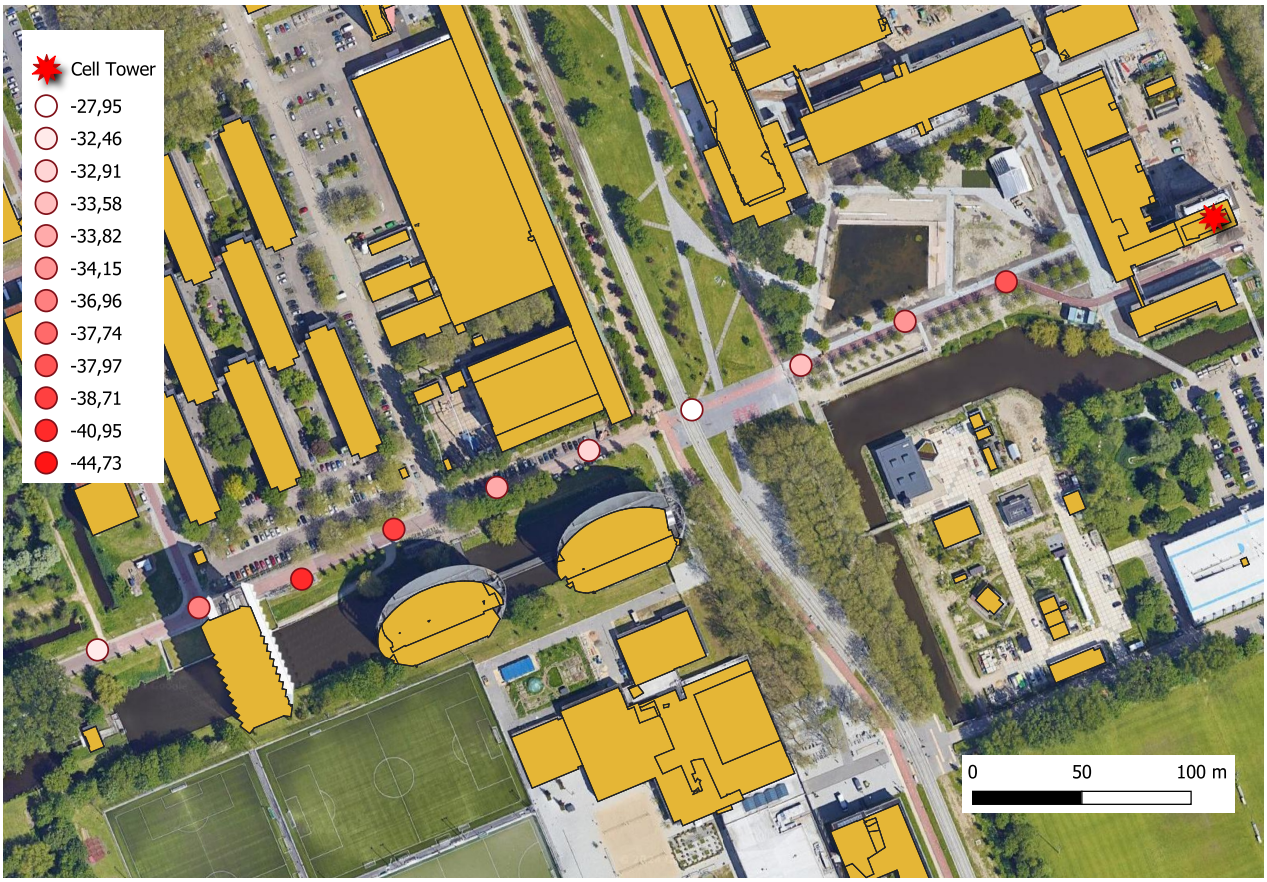

Figure 4.15: RSSI measurements showing signal strength variations due to tree obstructions (example 1).

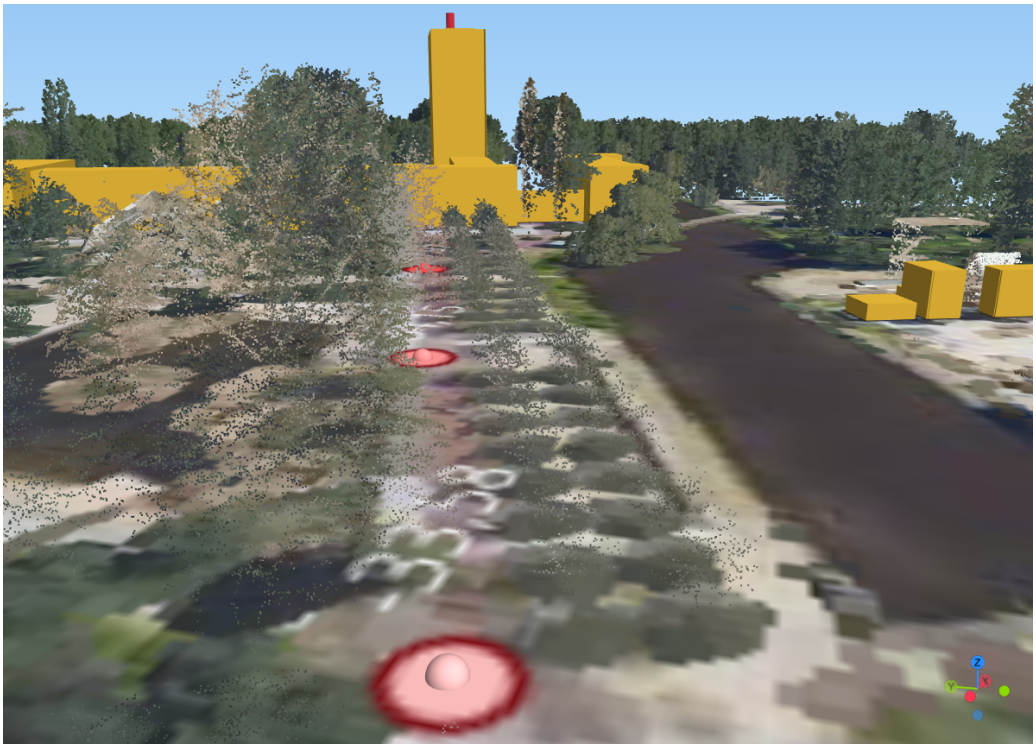

Figure 4.16: Signal strength variations due to tree obstruction (1) (example 1).

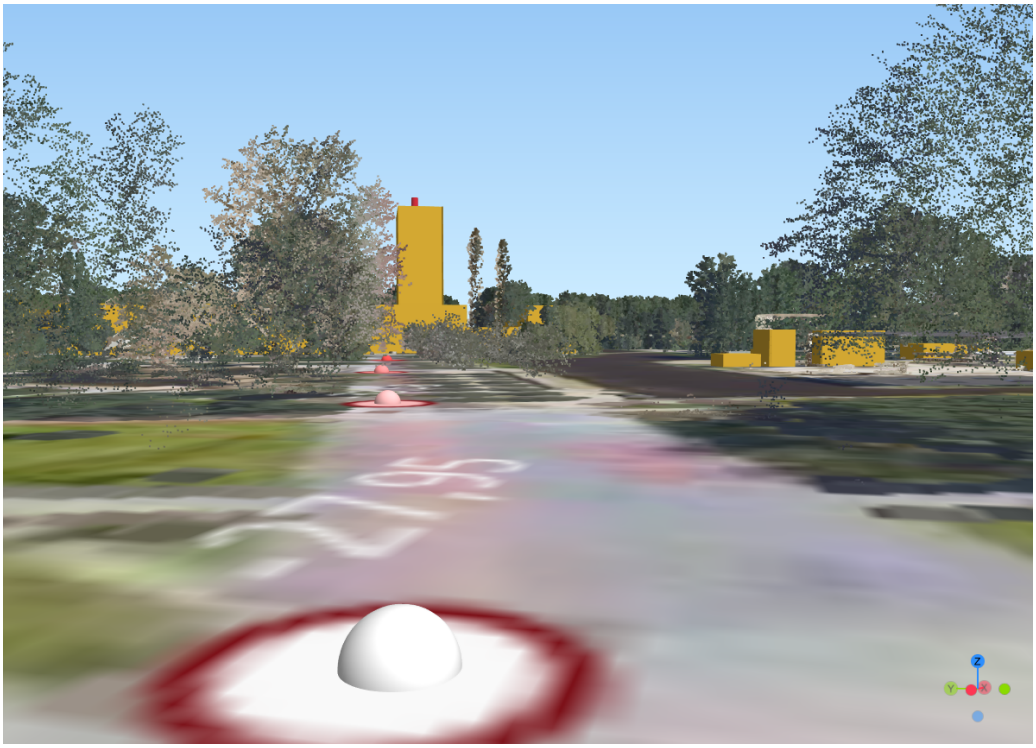

Figure 4.17: Signal strength variations due to tree obstruction (2) (example 1).

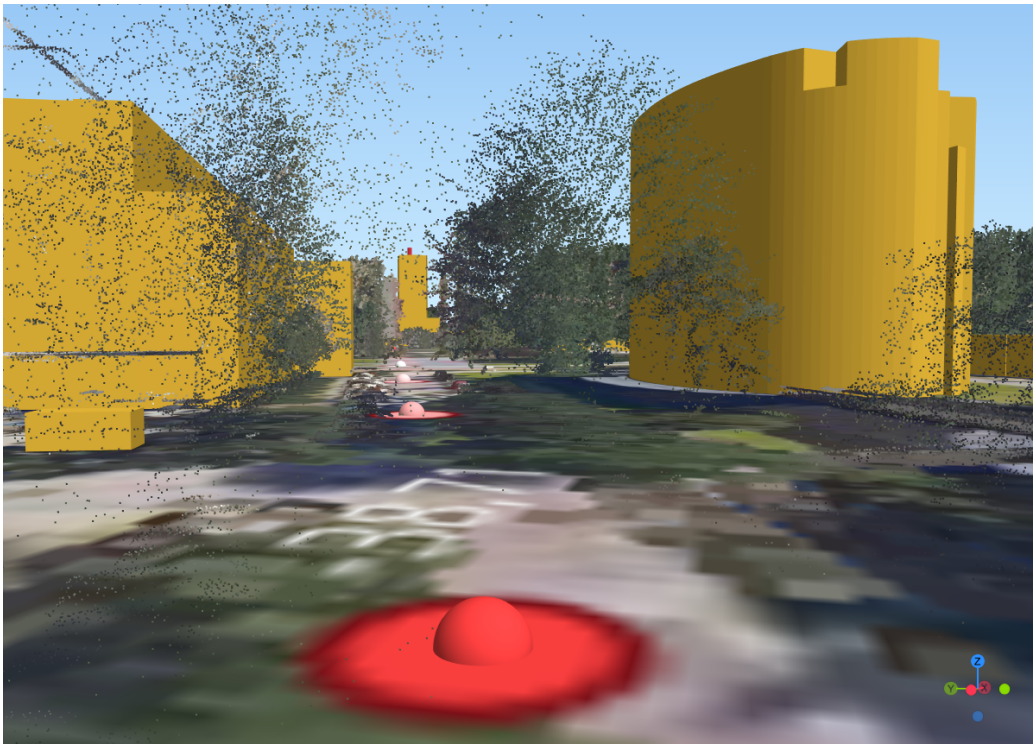

Figure 4.18: Signal strength variations due to tree obstruction (3) (example 1).

The impact of vegetation on 5G signal attenuation is further highlighted in a second example, which offers one more clear demonstration due to the absence of buildings or other obstacles in the environment. As expected, the signal strength was greater in areas with a clear line of sight to the cell tower with PCI 363, unimpeded by trees. Conversely, in areas where trees were present, the signal strength was notably reduced. Someone should take into

consideration that as anticipated, the signal strength also diminishes with increasing distance from the cell tower due to FSPL.

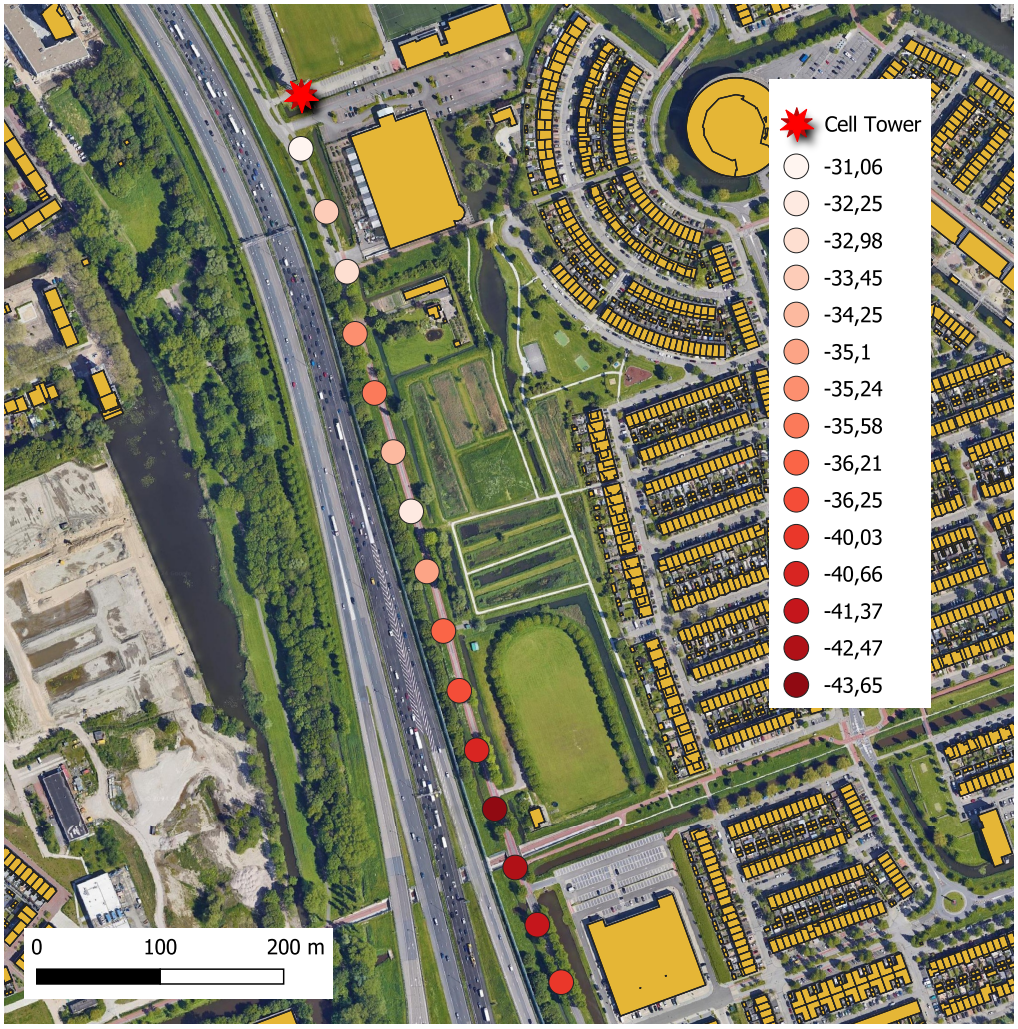

Figure 4.19: RSSI measurements showing signal strength variations due to tree obstructions (example 2).

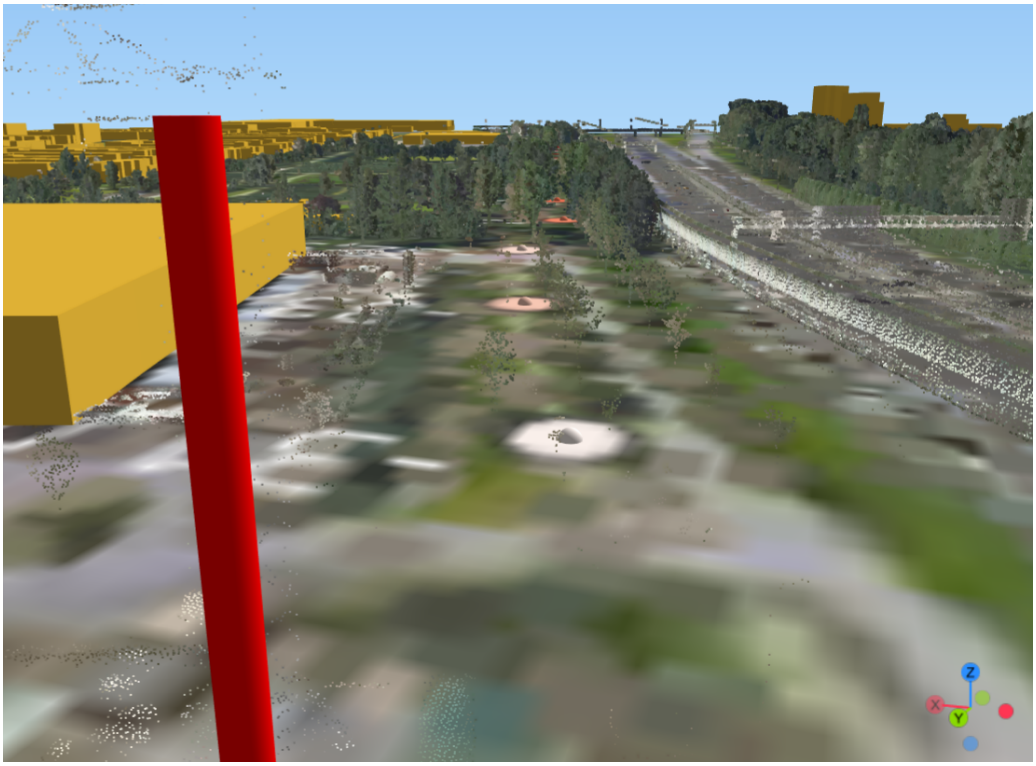

Figure 4.20: Signal strength variations due to tree obstruction (1) (example 2).

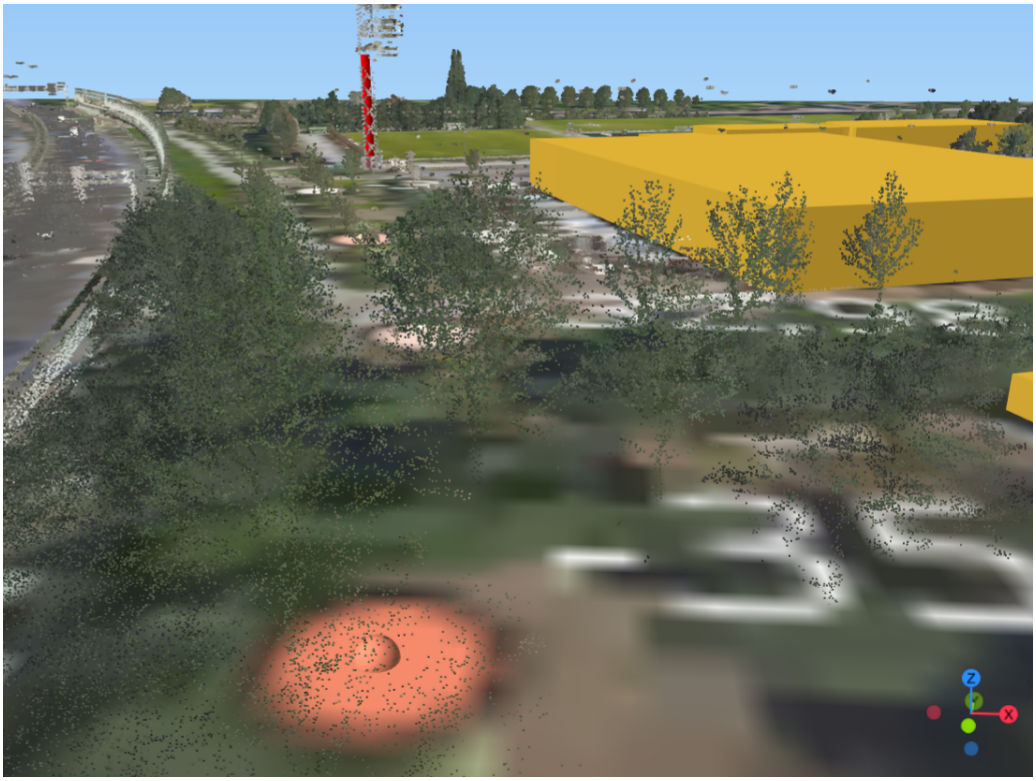

Figure 4.21: Signal strength variations due to tree obstruction (2) (example 2).

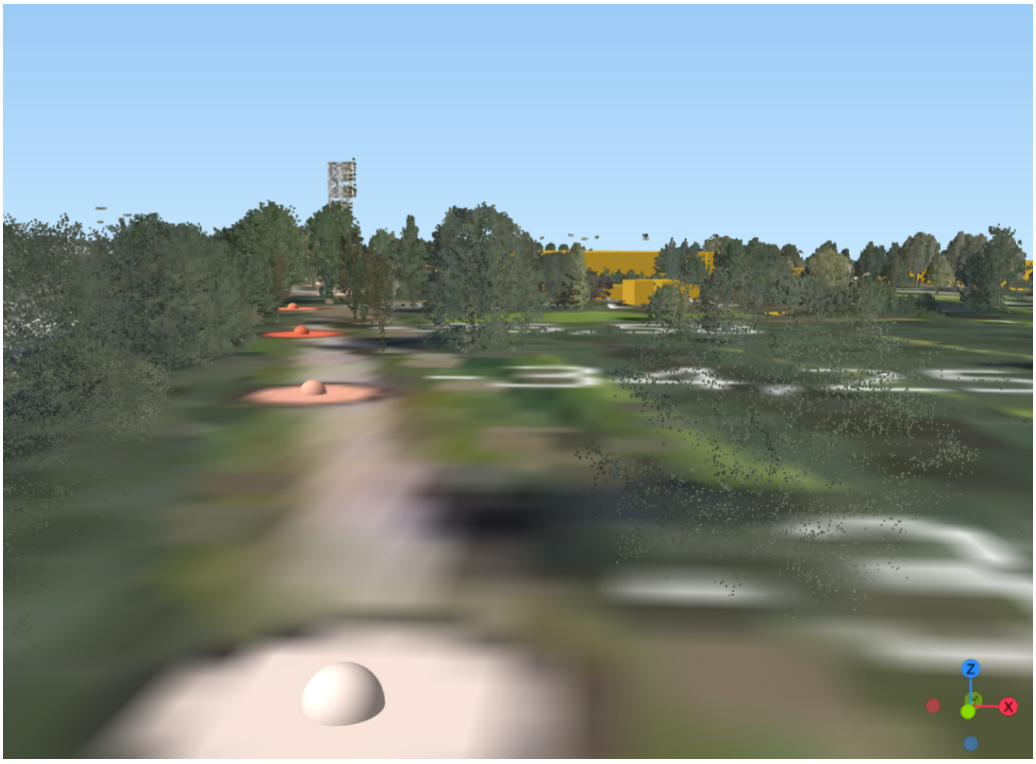

Figure 4.22: Signal strength variations due to tree obstruction (3) (example 2).

Figure 4.23: Signal strength variations due to tree obstruction (4) (example 2).

4.3 Effect of 5G Network Distribution on PDOP Accuracy

The research question "How is PDOP affected by the distribution of the 5G network?" is addressed through a detailed examination of how the network's layout influences positioning

accuracy, which relies on the ability of the modem to connect to multiple cell towers so as its precise location to be determined. However, there are instances where a device cannot receive signals from the necessary number of towers, impeding this process.

In urban areas where the density of 5G towers is higher, devices typically have no trouble connecting to more than three cell towers. They might also receive signals from different transmitters of the same cell tower. This dense network ensures that telecommunication goals are highly achieved, as devices can easily gather the required signals. However, there are certain locations where devices cannot obtain signals from the necessary number of towers impacting on their ability to perform trilateration, leading to less accurate positioning(Del Peral-Rosado et al., 2018).

During the 20-minute static measurements that were performed, only two cell towers were identified in certain locations. This inability to connect to more than two towers hindered the performance of trilateration. One of these locations is presented in Figure 4.24 (The finding is presented in Google Earth as the *3DBAG* dataset is not yet updated for some of the buildings around the observation point).

Figure 4.24: Observation point where the signal from only two cell towers was retrieved during static measurements.

The location is inside TU Delft campus near the Echo building. However, several tall buildings nearby likely block the network signal. As a result, the received signals were mainly from the closest cell towers, 198 meters away. Fewer signals were also received from only one other tower.
As described in Section 2.4 and confirmed in Section 4.2 the presence of obstacles (like buildings, vegetation, etc.) between base stations and the user can cause signal degradation and affect accuracy. For instance, especially in urban environments with many tall buildings can cause reflections and multipath effects. Increasing the density of cell towers within a 5G

network enhances the accuracy of position determination by providing a greater number of reference points for trilateration. A well-distributed network minimizes the presence of obstacles between the device and the cell towers, reducing signal degradation. Consequently, the signal quality remains high, leading to more accurate and reliable position estimates.

Finally, the closer the device is to a cell tower, the lower the error in the calculated distance through RSSI from the actual distance is. This proximity reduces the impact of signal attenuation and interference, resulting in more accurate distance measurements. This is confirmed in Figure 4.25 that shows the error of the calculated distance from the observation point to the cell tower against the real distance.

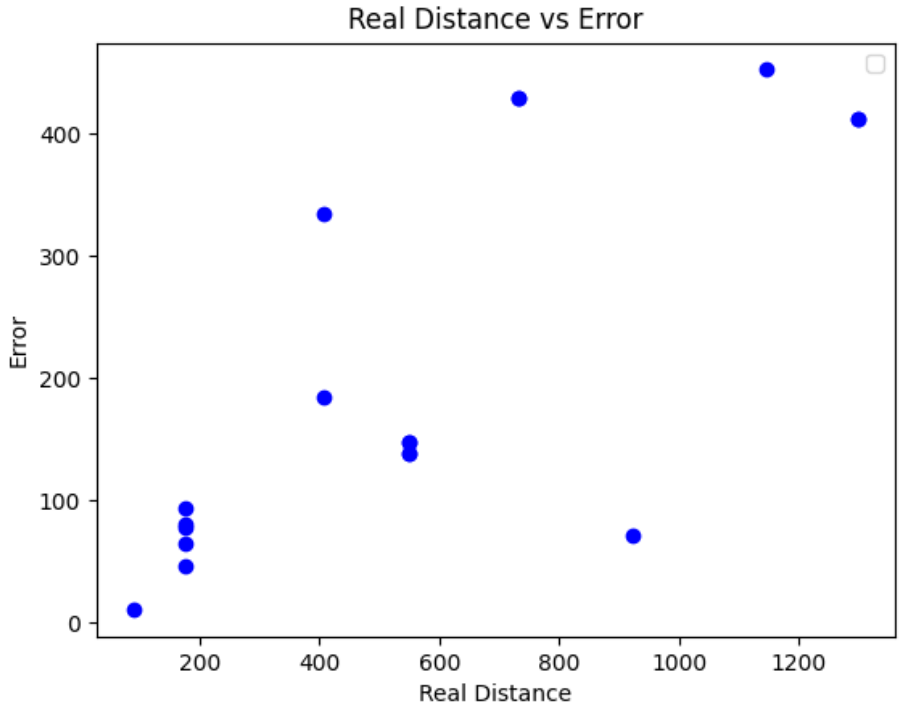

Figure 4.25: Error of the calculated distance through RSSI values against the real distance.

Accurately categorizing locations and specifying the exact distances required for optimal 5G signal reception remains a complex challenge due to the variability in environmental conditions and the limited number of measurements. To address these challenges, more comprehensive data collection and advanced modeling techniques are necessary.

In addition, as mentioned in Section 2.9, the geometric configuration of the antennas plays an important role in positioning using the trilateration method. When the geometric configuration is poor, such as when the antennas are nearly collinear or too close to each other, the accuracy of the position estimation decreases. This effect is confirmed in the results produced by the *MOVE3* software, as shown in Figure 4.26. When the observation point lies within a well-formed triangle created by the antennas, the accuracy improves significantly. In the following scenarios, the antennas remain in the same position, but the observation point is moved outside the "triangle." The ellipses that represent the estimated error of the position of the observation point clearly illustrate the difference in accuracy.

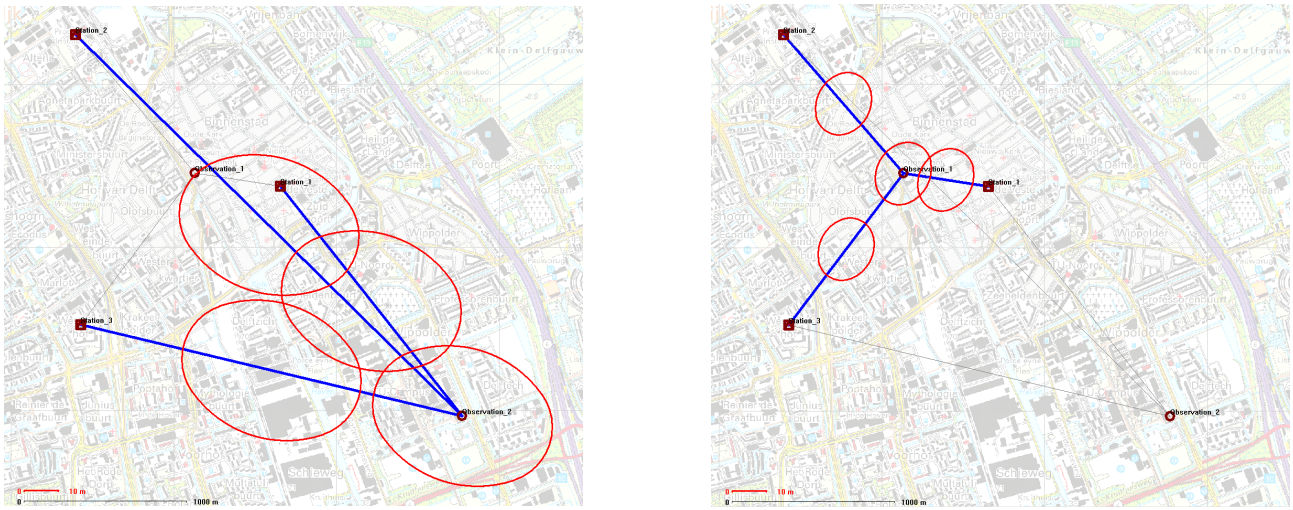

Figure 4.26: PDOP distribution when the observation point is outside the triangle that the antennas form (left image) and when it is outside (right image).

A similar example depicted in Figure 4.27. Although the observation point remains the same in both cases and is connected to three cell towers, exhibits higher accuracy compared to the right. Specifically, in the right image, where the cell towers are arranged in a collinear manner, the ellipses are larger and more elongated, taking on an oval shape. In contrast, in the left image, where the cell towers form a triangular configuration around the observation point, the ellipses appear more circular. This is because the more favorable geometry of the towers reduces PDOP, leading to higher positioning accuracy.

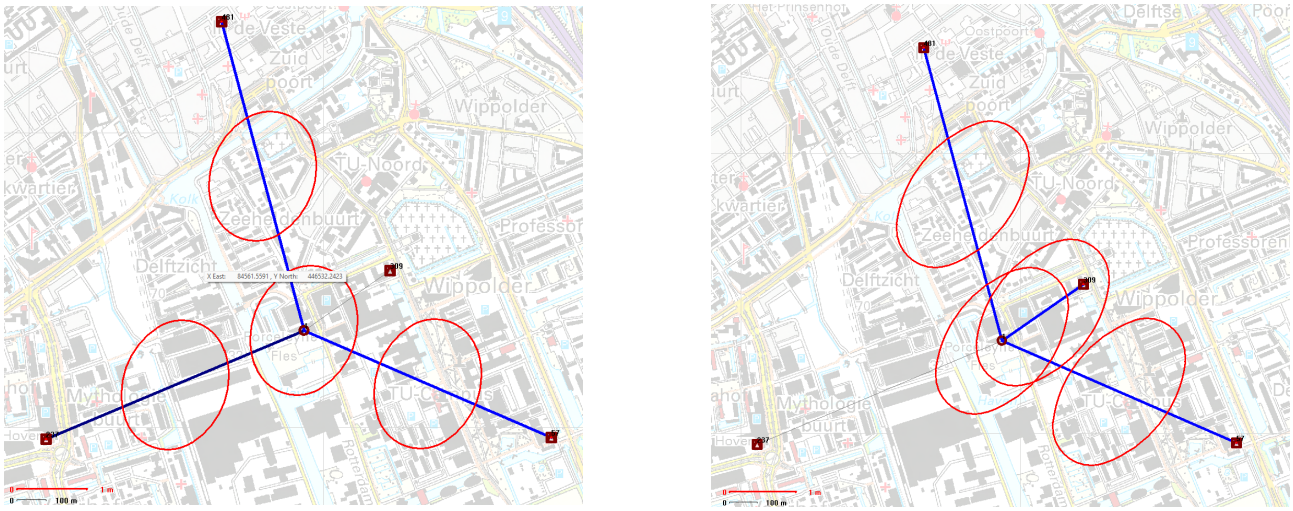

Figure 4.27: PDOP distribution when the connected cell towers form a triangle and the observation point lies in that (left image) in comparison to when they are collinear (right image).

Chapter 5

Conclusions & Recommendations

5.1 Conclusions

The RSSI measurements obtained with different antenna types showed considerable variability. The performance of each antenna type influenced the RSSI readings, which highlights the importance of selecting appropriate antennas to ensure more consistent signal measurements and accurate positioning. However, the variability is approximately the same with all the tested antennas.

Tests on FSPL along a direct line of sight with a single antenna type revealed substantial fluctuations in RSSI values. These variations did not align with the expected logarithmic trend of FSPL models, indicating significant difficulties in accurately modeling path loss based on RSSI in practical conditions.

RSSI values exhibited irregular fluctuations, including occasional increases at specific distances. This unpredictability complicates the direct correlation between RSSI and distance, making it difficult to derive precise distance estimates solely from RSSI measurements. Factors such as environmental conditions and interference contribute to these variations.

Attempts to determine position using trilateration based on averaged RSSI values at various locations resulted in position estimates that significantly deviated from actual points. The large uncertainty observed in the positional estimates indicates that RSSI-based trilateration is currently imprecise, with high spatial uncertainty.

While RSSI measurements provide useful information about other applications, their inherent variability and unpredictability present challenges for accurate positioning. The difficulties encountered in FSPL modeling and the substantial errors in trilateration results suggest a need for alternative or complementary methods to improve positioning accuracy.

One of the primary objectives of this research is to explore 5G RSSI-based positioning as an alternative solution in environments where GNSS is compromised, such as urban canyons. However, the findings indicate that in certain urban scenarios, not only the presence of buildings or other topographic factors that can obstruct or attenuate 5G signals but also, the current geometric configuration of 5G cell towers can result in the reception of signals from fewer than three cell towers. This issue further complicates the highly accurate positioning process for RSSI-based positioning as well as the other 5G positioning methods (e.g. AOA, TDoA, MC-RTT).

The geometric configuration of cell towers is a critical factor in determining the accuracy of

positioning in 5G networks using trilateration. When towers form a well-distributed triangle around the observation point, the PDOP is lower, resulting in more accurate position estimates with smaller, more circular ellipses. In contrast, poor geometric configurations, such as collinear or closely clustered towers, increase PDOP leading to larger and more elongated error ellipses, reflecting greater uncertainty. This demonstrates that favorable cell tower arrangements significantly enhance positioning accuracy, while unfavorable configurations degrade it, making geometry a key factor in 5G network design for precise location services.

5.2 Answer to Research Question

Some research sub-questions were addressed to provide necessary insights foundation for answering the main research question. The answers to them are described below:

- **What is the potential accuracy of standalone 5G positioning with the trilateration method in comparison to the "ground truth" provided by GNSS-RTK?**

  The potential accuracy of standalone 5G positioning using the trilateration method is limited and imprecise. Measurements showed significant variability in RSSI values, leading to spatial uncertainty in position estimates. Even after applying trilateration, the calculated positions deviated hundreds of meters from the actual observation points. This high degree of uncertainty makes RSSI-based trilateration less reliable when compared to GNSS-RTK, which can achieve centimeter-level precision under favorable conditions. The variability and unpredictability of RSSI hinder accurate distance estimation and positioning.

- **What is the impact of topographic factors (e.g. buildings, urban canyons) on the accuracy of 5G positioning?**

  Topographic factors like buildings and vegetation can severely impact the accuracy of 5G positioning by obstructing or attenuating signals. Trees, buildings, and other obstacles cause reflections, diffractions and scattering of 5G signals, which lead to variations in RSSI. For instance, RSSI values tend to drop in areas with trees or obstructions between the device and the cell tower. In urban canyons with many buildings reflections and multipath effects further degrade positioning accuracy. This is evident from the irregular fluctuations in RSSI and signal degradation observed in areas with significant obstacles.

- **How is the PDOP affected by the distribution of the 5G network?**

  The PDOP in 5G positioning is highly influenced by the geometric arrangement of the cell towers. When cell towers form a well-distributed triangular configuration around the observation point, the PDOP is lower, resulting in more accurate and circular positional error ellipses this is visualized through *MOVE3* software. However, when the towers are collinear or closely clustered, the PDOP increases, leading to larger and more elongated error ellipses, which signify greater uncertainty and less accurate positioning. A denser network of well-distributed cell towers helps reduce PDOP and improve positioning accuracy.

By exploring these aspects, the overall potential of the trilateration method using 5G RSSI for positioning accuracy can be evaluated. This evaluation comes to answer the main research question of this thesis which is: "To what extent can the trilateration method for positioning, utilizing only the RSSI of the 5G network, serve?". The results of this project showed that in

comparison to the "ground truth" provided by GNSS-RTK positioning, which offers centimeter level accuracy in most cases, 5G positioning using RSSI and trilateration is significantly less accurate. The method is only suitable for scenarios where rough estimates of location are sufficient. It could serve as a complementary or fallback system in areas where GNSS signals are unavailable, but its standalone precision is inadequate for high-accuracy applications.

5.3 Self Reflection

From the outset, it was apparent that depending only on RSSI measurements for accurate positioning might be problematic due to the inherent variability and unpredictability of signal strength. Despite this foresight, the detailed investigation into RSSI provided invaluable insights into the complexities of signal-based positioning systems. This research underscored the significant challenges associated with RSSI readings, such as their sensitivity to environmental factors and the difficulty in modeling path loss accurately. This approach reflects the importance of applying a formal, theoretical, and methodologically sound process to store, manage, and disseminate geo-data, as well as being at the forefront of data analysis methodology in positioning systems.

The findings of this study have significant implications beyond the technical scope. In the context of geomatics, accurate positioning and mapping are crucial for various applications, including urban planning, navigation, and environmental monitoring. This is especially true for indoor positioning and industrial navigation, where GNSS is unavailable and reliable methods are vital for operational success. The observed inaccuracies in RSSI-based positioning highlight the necessity for more reliable methods or complementary technologies to achieve better precision. This realization motivates the pursuit of innovative solutions and technologies that can enhance the reliability of positioning systems. This realization motivates the pursuit of innovative solutions and technologies that can enhance the reliability of positioning systems, further supporting the design and implementation of spatio-temporal models and systems for complex real-world situations.

From a societal perspective, the ability to improve positioning accuracy can have transformative effects. For example, in emergency services, accurate geolocation data can be crucial for effective response times, aligning with the knowledge gained the past 2 years regarding the understanding of geo-information's role in decision making in the built environment. Similarly, in urban development, precise positioning supports better infrastructure planning, contributing to efficiency and safety. The ability to address the challenges encountered in RSSI measurements aligns with the broader goal of applying geo-information to improve societal safety, operational efficiency, and long-term sustainability.

5.4 Future Work

Given the limitations identified in this study regarding RSSI measurements and their impact on positioning accuracy, several avenues for future research and development could be pursued to enhance the reliability and precision of spatial systems. For example, investigating the other 5G positioning methods, such as the AOA, AOD or the TDoA, which might offer greater accuracy and reduced susceptibility to environmental variability compared to RSSI. Combining multiple technologies could also improve positioning reliability through fusion of different data sources.

While RSSI is often viewed as less accurate compared to the other 5G positioning methods, future studies could focus on exploring how 5G's unique characteristics such as dense small-cell deployments, beamforming and mmWave frequencies can enhance RSSI-based positioning. Additionally, conducting comprehensive studies to investigate methods to mitigate common RSSI issues such as signal attenuation, multipath interference, or environmental noise caused by building materials, weather conditions, or urban density . Techniques like calibration, filtering, or even machine learning could be employed to refine RSSI measurements and improve their reliability.

A valuable next step would be to develop a detailed DOP map of Delft, displaying the DOP value for every location within the city. Since positioning accuracy is determined by the equation

$$\text{Position Accuracy} = \text{UERE} * \text{DOP} \tag{5.1}$$

where User Equivalent Range Error (UERE) represents the error in the distance between a transmitter and the user's receiver (Kaplan and Hegarty, 2006). This map could serve as a powerful tool to assess potential positioning accuracy throughout the area. If signal strength errors were eliminated, the DOP map could be generated based solely on the known locations of cell towers and their transmitted power, allowing for more accurate predictions of RSSI at specific distances from each tower. This would provide a clearer understanding of how the geometric distribution of cell towers affects the precision of 5G-based positioning.

Finally, a promising and intriguing aspect of 5G positioning is its potential for indoor positioning. Utilizing floor plans or reference points within indoor environments, researchers can apply similar measurement techniques and methodologies as employed in this study to derive positioning results. The presence of smaller antennas or signal boosters within buildings could enhance the performance and accuracy of RSSI-based positioning systems. By strategically placing these devices, it may be possible to mitigate some of the challenges associated with signal variability and interference, thereby improving the reliability of indoor positioning solutions. Future research should explore these possibilities, as the controlled environment of indoor spaces might offer more consistent and predictable signal behavior, contributing to more precise and dependable positioning outcomes.

Appendix A

Tools and Datasets

A.1 Ublox C099-F9P (GNSS-RTK device)

The Ublox C099-F9P[1] application board facilitates the effective assessment of the ZED-F9P, u-blox's high-precision positioning module. The ZED-F9P module offers multi-band GNSS positioning and incorporates built-in RTK technology, delivering centimeter-level accuracy. The application board, C099-F9P, integrates the ZED-F9P module and includes an ODIN-W2 short-range module for connectivity options. Designed to support ZED-F9P module evaluation, the ODIN-W2 module adds wireless connectivity.

The u-center software is the platform for assessing u-blox GNSS receivers. Through u-center, data can be both logged and visualized in real-time. Additionally, the u-center software features an Networked Transport of RTCM via Internet Protocol (NTRIP) server/client, enabling the management of the RTCM correction stream to and from a C099-F9P application board.

The kit includes (Figure A.1):

- Application board with ZED-F9P
- Active multi-band GNSS antenna
- Bluetooth / Wi-Fi antenna
- USB cable

[1] https://www.u-blox.com/en/product/c099-f9p-application-board

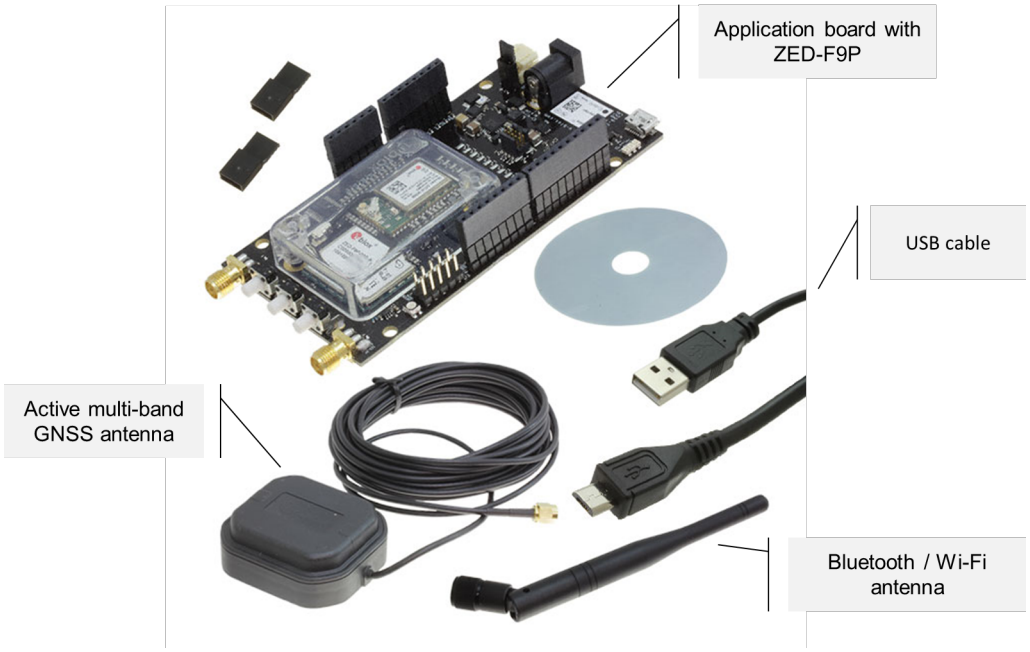

Figure A.1: Ublox C099-F9P components - GNSS-RTK device.

A.2 Quectel RM520N-GL (M.2 device)

Quectel RM520N-GL[2] [3] (Figure A.2 is an Internet of Things (IoT) and eMBB module specifically crafted for 5G sub-6GHz applications. It incorporates 3GPP[4] Release 16 technology, enabling support for both 5G Non-Standalone (NSA) and standalone (SA) modes.

The USB TO M.2 B KEY is as a module driver board designed to interface with M.2 modules for 5G connectivity. The measurements were performed with three different types of antennas (see Figure A.3).

(a) RM520N-GL (b) USB TO M.2 B KEY

Figure A.2: Quectel RM520N-GL (M.2 device) - 5G modem.

[2] https://www.waveshare.com/wiki/RM520N-GL
[3] https://www.waveshare.com/wiki/USB_TO_M.2_B_KEY
[4] https://www.3gpp.org/

(a) Type 1 (b) Type 2 (c) Type 3

Figure A.3: Different types of antennas.

A.3 *MOVE3* Software

Figure A.4: *MOVE3* software.

MOVE3[5] is a software designed for geodetic professionals, offering advanced features for the design, adjustment, and quality control of geodetic networks in one, two and three dimensions. *MOVE3* provides a robust platform for processing both GNSS and terrestrial observations using 'Total Station' measurements (Sweco, 2024).

One of *MOVE3*'s standout features is its adherence to a true 3D mathematical model, ensuring accurate handling of complex ellipsoidal coordinate estimation without resorting to spherical or planar approximations (Sweco, 2024).

It offers a user-friendly userface, equipped with tools such as automatic computation of approximate coordinates and sophisticated error detection mechanisms to enhance efficiency and accuracy. Its adaptability allows for the integration of various geodetic observation types, enabling the construction of networks tailored to specific requirements. Importantly, *MOVE3* prioritizes productivity by identifying potential errors during data analysis, thereby minimizing the need of costly troubleshooting and re-measurement. The software's intuitive design and robust functionality contribute to increased productivity and meaningful time savings, making it a valuable tool for geodetic professionals (Sweco, 2024).

A.4 Excel file of *Vodafone* Network Cell Towers

Through CGI's collaboration with *Vodafone Ziggo*, we were able to request information regarding the cell towers of the network. An Excel file was provided containing details for each antenna located around two specific sites: one in Delft and another in Rotterdam. Specifically, the known data for each PCI is:

- eNB ID
- eNB Name
- SiteNr
- Longitude
- Latitude
- Altitude
- Height
- Site Type
- i/o TYPE
- In-Service
- OP/Vendor
- eNB Image
- Label Location
- EARFCN

[5] https://move3software.com/

- PCI
- PCI Mod
- Band
- Azimuth
- Angle
- Frequency
- TAC
- Cell ID
- Sector ID
- Gain
- Tx Power
- Ant. Name
- Mech. Tilt
- Elec. Tilt
- Neighbor
- Sector Image

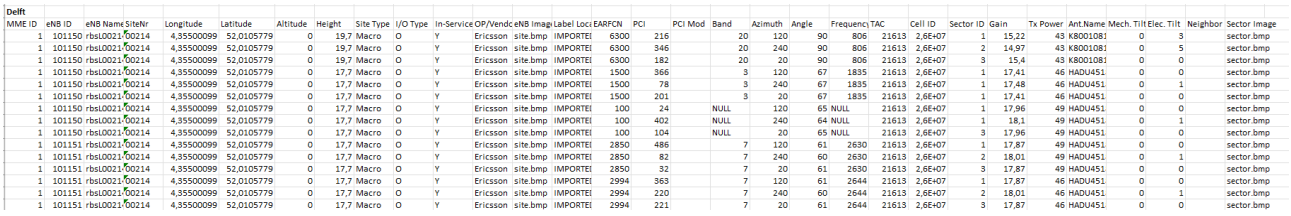

Delft																														
MME ID	eNB ID	eNB Name	SiteNr	Longitude	Latitude	Altitude	Height	Site Type	I/O Type	In-Service	OP/Vendo	eNB Imag	Label Loca	EARFCN	PCI	PCI Mod	Band	Azimuth	Angle	Frequency	TAC	Cell ID	Sector ID	Gain	Tx Power	Ant.Name	Mech. Tilt	Elec. Tilt	Neighbor	Sector Image
1	101150	rbsL0021	00214	4,35500099	52,0105779	0	19,7	Macro	O	Y	Ericsson	site.bmp	IMPORTEI	6300	216		20	120	90	806	21613	2,6E+07	1	15,22	43	K8001081	0	3		sector.bmp
1	101150	rbsL0021	00214	4,35500099	52,0105779	0	19,7	Macro	O	Y	Ericsson	site.bmp	IMPORTEI	6300	346		20	240	90	806	21613	2,6E+07	2	14,97	43	K8001081	0	5		sector.bmp
1	101150	rbsL0021	00214	4,35500099	52,0105779	0	19,7	Macro	O	Y	Ericsson	site.bmp	IMPORTEI	6300	182		20	20	90	806	21613	2,6E+07	3	15,4	43	K8001081	0	0		sector.bmp
1	101150	rbsL0021	00214	4,35500099	52,0105779	0	17,7	Macro	O	Y	Ericsson	site.bmp	IMPORTEI	1500	366		3	120	67	1835	21613	2,6E+07	1	17,41	46	HADU451	0	0		sector.bmp
1	101150	rbsL0021	00214	4,35500099	52,0105779	0	17,7	Macro	O	Y	Ericsson	site.bmp	IMPORTEI	1500	78		3	240	67	1835	21613	2,6E+07	1	17,48	46	HADU451	0	1		sector.bmp
1	101150	rbsL0021	00214	4,35500099	52,0105779	0	17,7	Macro	O	Y	Ericsson	site.bmp	IMPORTEI	1500	201		3	20	67	1835	21613	2,6E+07	1	17,41	46	HADU451	0	0		sector.bmp
1	101150	rbsL0021	00214	4,35500099	52,0105779	0	17,7	Macro	O	Y	Ericsson	site.bmp	IMPORTEI	100	24		NULL	120	65	NULL	21613	2,6E+07	1	17,96	49	HADU451	0	0		sector.bmp
1	101150	rbsL0021	00214	4,35500099	52,0105779	0	17,7	Macro	O	Y	Ericsson	site.bmp	IMPORTEI	100	402		NULL	240	64	NULL	21613	2,6E+07	1	18,1	49	HADU451	0	1		sector.bmp
1	101150	rbsL0021	00214	4,35500099	52,0105779	0	17,7	Macro	O	Y	Ericsson	site.bmp	IMPORTEI	100	104		NULL	20	65	NULL	21613	2,6E+07	3	17,96	49	HADU451	0	0		sector.bmp
1	101151	rbsL0021	00214	4,35500099	52,0105779	0	17,7	Macro	O	Y	Ericsson	site.bmp	IMPORTEI	2850	486		7	120	61	2630	21613	2,6E+07	1	17,87	49	HADU451	0	0		sector.bmp
1	101151	rbsL0021	00214	4,35500099	52,0105779	0	17,7	Macro	O	Y	Ericsson	site.bmp	IMPORTEI	2850	82		7	240	60	2630	21613	2,6E+07	2	18,01	49	HADU451	0	1		sector.bmp
1	101151	rbsL0021	00214	4,35500099	52,0105779	0	17,7	Macro	O	Y	Ericsson	site.bmp	IMPORTEI	2850	32		7	20	61	2630	21613	2,6E+07	3	17,87	49	HADU451	0	0		sector.bmp
1	101151	rbsL0021	00214	4,35500099	52,0105779	0	17,7	Macro	O	Y	Ericsson	site.bmp	IMPORTEI	2994	363		7	120	61	2644	21613	2,6E+07	1	17,87	46	HADU451	0	0		sector.bmp
1	101151	rbsL0021	00214	4,35500099	52,0105779	0	17,7	Macro	O	Y	Ericsson	site.bmp	IMPORTEI	2994	220		7	240	60	2644	21613	2,6E+07	2	18,01	46	HADU451	0	1		sector.bmp
1	101151	rbsL0021	00214	4,35500099	52,0105779	0	17,7	Macro	O	Y	Ericsson	site.bmp	IMPORTEI	2994	221		7	20	61	2644	21613	2,6E+07	3	17,87	46	HADU451	0	0		sector.bmp

Figure A.5: Excel file with information for each *Vodafone Ziggo* 5G cell tower.

A.5 Qgis2threejs (QGIS plugin)

Figure A.6: Qgis2threejs (QGIS plugin).

Qgis2threejs is a plugin for Quantum Geographic Information System (QGIS) that enables the creation of interactive 3D visualizations from 2D Geographic Information System (GIS) data. It supports various data types, including vector and raster data, allowing for detailed 3D representations of geographic features and terrain. The plugin integrates seamlessly with QGIS, offering a user-friendly interface for customizing and exporting 3D models as web pages using WebGL, which can be viewed and shared in any compatible web browser. This functionality enhances spatial data analysis and presentation, making complex geographic relationships easier to understand and communicate QGIS, 2024.

A.6 3DBAG

3DBAG stands for "3D Basisregistratie Adressen en Gebouwen", which translates to "3D Basic Registration of Addresses and Buildings". The *3DBAG* is a comprehensive dataset featuring 3D building models for the Netherlands, created by combining *BAG* building data and *AHN* height data. These models, available in various levels of detail, are regularly updated to reflect the latest information. The dataset is used for numerous applications, including urban planning, environmental simulations, and noise pollution analysis. Developed by the 3D Geoinformation research group 3D Geoinformation Research Group, 2024.

A.7 AHN4

The *AHN4*, or "Actueel Hoogtebestand Nederland 4," is the fourth iteration of the digital elevation model for the Netherlands. This dataset is collected through airborne laser scanning Light Detection And Ranging (LiDAR) and provides highly detailed and precise altitude data. The *AHN* project, carried out between 2020 and 2022, includes multiple elevation measurements per square meter, with an average point density of approximately 10 points per square meter, ensuring a high level of detail for various applications such as water management, infrastructure planning, and environmental monitoring AHN, 2024

A.8 Google Earth

Google Earth is a virtual globe application that lets users explore a 3D representation of Earth. Someone is able to zoom in on specific locations, view satellite imagery, and explore maps, terrain and 3D buildings. It is a great tool for getting a visual perspective of different parts of the world, whether someone is checking out their own neighborhood or exploring far-off places (Google, 2024).

Bibliography

3D Geoinformation Research Group, D. U. o. T. (2024). 3DBAG: 3D building models of the Netherlands [Accessed: 2024-07-10]. https://docs.3dbag.nl/en/

Afroz, F., Subramanian, R., Heidary, R., Sandrasegaran, K., & Ahmed, S. (2015). SINR, RSRP, RSSI and RSRQ measurements in long term evolution networks. *International Journal of Wireless & Mobile Networks*, *7*, 113–123. https://doi.org/10.5121/ijwmn.2015.7409

Ahmad, A., Hasan, S., & Majeed, S. (2019). 5G mobile systems, challenges and technologies: A survey. *Journal of Theoretical and Applied Information Technology*, *97*, 3214–3226. https://doi.org/10.5281/zenodo.3256485

AHN. (2024). AHN - Actueel Hoogtebestand Nederland [Maintained by Het Waterschapshuis, which can be found at https://www.waterschaphuis.nl]. https://www.ahn.nl

Alghisi, M., & Biagi, L. (2023). Positioning with GNSS and 5G: Analysis of geometric accuracy in urban scenarios. *Sensors*, *23*(4). https://doi.org/10.3390/s23042181

Ali, E., Ismail, M., Nordin, R., & Abdulah, N. F. (2017). Beamforming techniques for massive MIMO systems in 5G: Overview, classification, and trends for future research. *Frontiers of Information Technology & Electronic Engineering*, *18*(6), 753–772. https://doi.org/10.1631/FITEE.1601817

Ali, S., Abu-Samah, A., Abdullah, N. F., & Mohd Kamal, N. L. (2024). Propagation modeling of unmanned aerial vehicle (UAV) 5G wireless networks in rural mountainous regions using ray tracing. *Drones*, *8*(7). https://doi.org/10.3390/drones8070334

Alimi, I. A., Patel, R. K., Muga, N. J., & Monteiro, P. P. (2020). Performance analysis of 5G fixed wireless access networks with antenna diversity techniques. *Wireless Personal Communications*, *113*(3), 1541–1565. https://doi.org/10.1007/s11277-020-07399-8

Baarda, W. (1968). *A testing procedure for use in geodetic networks* (Vol. 2). Rijkscommissie voor Geodesie.

Cardoso, K. V., Both, C. B., Prade, L. R., Macedo, C. J. A., & Lopes, V. H. L. (2020). A softwarized perspective of the 5G networks.

Chen, L., Zheng, F., Gong, X., & Jiang, X. (2023). GNSS high-precision augmentation for autonomous vehicles: Requirements, solution, and technical challenges. *Remote Sensing*, *15*, 1623. https://doi.org/10.3390/rs15061623

Del Peral-Rosado, J. A., Saloranta, J., Destino, G., López-Salcedo, J. A., & Seco-Granados, G. (2018). Methodology for simulating 5G and GNSS high-accuracy positioning. *Sensors*, *18*(10). https://doi.org/10.3390/s18103220

Elshaer, H., Boccardi, F., Dohler, M., & Irmer, R. (2014). Downlink and uplink decoupling: A disruptive architectural design for 5G networks. https://doi.org/10.1109/GLOCOM.2014.7037069

Feng, Y., & Wang, J. (2008). GPS RTK performance characteristics and analysis. *Journal of Global Positioning Systems*, *7*. https://doi.org/10.5081/jgps.7.1.1

Geo++. (2023). *The "accuracy in real-time" problem*. Retrieved January 9, 2024, from https://www.geopp.de/ssr-vs-osr/

Google. (2024). *Google earth* [Accessed: 2024-07-29]. https://earth.google.com

Groves, P. D. (2013). *Principles of GNSS, inertial, and multisensor integrated navigation systems*. Artech House.

Gunnarsson, F., & Shreevastav, R. (2022). *3GPP GNSS positioning and integrity: The latest trials and developments*. Telefonaktiebolaget LM Ericsson. Retrieved January 9, 2024, from https://www.ericsson.com/en/blog/2022/5/gnss-positioning-integrity-3gpp

Hexagon. (2023). *An introduction to GNSS* (3rd). NovAtel Inc.

Humphreys, T. E., Ledvina, B. M., Psiaki, M. L., O'Hanlon, B. W., & Kintner, P. M. (2008). Assessing the spoofing threat: Development of a portable GPS civilian spoofer. *Proceedings of the 21st International Technical Meeting of the Satellite Division of The Institute of Navigation (ION GNSS 2008)*, 2314–2325.

Islam, S. K., & Haider, M. R. (2010). *Sensors and low power signal processing*. Springer New York.

Ismail, M. I. M., Dzyauddin, R. A., Samsul, S., Azmi, N. A., Yamada, Y., Yakub, M. F. M., & Salleh, N. A. B. A. (2019). An RSSI-based wireless sensor node localisation using trilateration and multilateration methods for outdoor environment. https://arxiv.org/abs/1912.07801

Kaplan, E. D., & Hegarty, C. J. (2006). *Understanding gps: Principles and applications* (2nd). Artech House.

Keating, R., Säily, M., Hulkkonen, J., & Karjalainen, J. (2019). Overview of positioning in 5G new radio. *2019 16th International Symposium on Wireless Communication Systems (ISWCS)*, 320–324. https://doi.org/10.1109/ISWCS.2019.8877160

Langley, R. B. (1999). Dilution of precision. https://api.semanticscholar.org/CorpusID:16850160

Liu, Y., Shi, X., He, S., & Shi, Z. (2017). Prospective positioning architecture and technologies in 5G networks. *IEEE Network*, *31*(6), 115–121. https://doi.org/10.1109/MNET.2017.1700066

Mogyorósi, F., Revisnyei, P., Pašić, A., Papp, Z., Törös, I., Varga, P., & Pašić, A. (2022). Positioning in 5G and 6G networks - a survey. *Sensors (Basel)*, *22*(13), 4757. https://doi.org/10.3390/s22134757

Pileggi, C., Grec, F. C., & Biagi, L. (2023). 5G positioning: An analysis of early datasets. *Sensors (Basel)*, *23*(22), 9222. https://doi.org/10.3390/s23229222

QGIS. (2024). Qgis2threejs: A QGIS plugin for 3D visualization [Accessed: 2024-07-10]. https://plugins.qgis.org/plugins/Qgis2threejs/#plugin-about

Rydholm, C., & Pommer, W. (2021). Hybrid positioning solution using 5G and GNSS. https://api.semanticscholar.org/CorpusID:263699413

Shang, F., Su, W., Wang, Q., Gao, H., & Fu, Q. (2014). A location estimation algorithm based on RSSI vector similarity degree. *International Journal of Distributed Sensor Networks*, *10*(8), 371350. https://doi.org/10.1155/2014/371350

Speidel, J. (2021). Basic parameters of wireless transmission and multipath propagation. In *Introduction to digital communications* (pp. 63–85). Springer International Publishing. https://doi.org/10.1007/978-3-030-67357-4_5

Steffens, J. A. (2023). Libqmi: QMI modem protocol helper library (version 1.34.0-1) [Accessed: 2024-09-10]. https://www.freedesktop.org/wiki/Software/libqmi/

Sweco. (2024). *Move3 software*. Retrieved May 6, 2024, from https://move3software.com/

Sweco Nederland B.V. (2024). *Move3 user manual* (Version 4.6) [All rights reserved]. Sweco Nederland B.V.

Talvitie, J., Levanen, T., Koivisto, M., Ihalainen, T., Pajukoski, K., Renfors, M., & Valkama, M. (2018). Positioning and location-based beamforming for high speed trains in 5G NR networks. *2018 IEEE Globecom Workshops (GC Wkshps)*, 1–7. https://doi.org/10.1109/GLOCOMW.2018.8644311

Tiberius, C., van der Marel, H., Reudink, R., & van Leijen, F. (2022). *Surveying and mapping* [TU Delft OPEN Textbook]. TU Delft OPEN Publishing. https://doi.org/10.5074/T.2021.007

Verbree, E. (2023). GNSS code-observation positioning performance for the built environment [GEO1003 – 2023Q2].

Wabbena, G., Schmitz, M., & Bagge, A. (2005). PPP-RTK: Precise point positioning using state-space representation in RTK networks. *Proceedings of the 18th International Technical Meeting of the Satellite Division of The Institute of Navigation (ION GNSS 2005)*, 2584–2594.

Xia, S., Liu, Y., Yuan, G., Zhu, M., & Wang, Z. (2017). Indoor fingerprint positioning based on Wi-Fi: An overview. *ISPRS International Journal of Geo-Information*, *6*(5). https://doi.org/10.3390/ijgi6050135

Yuen, M. F. (2009, March). *Dilution of precision (DOP) calculation for mission planning purposes* [Master's thesis, Naval Postgraduate School]. https://www.nps.edu/Academics/AcademicDepartments/IS/Theses/YuenM2009.pdf

Colophon

This document was typeset using LaTeX. The main font is Roman (upright) serif.